



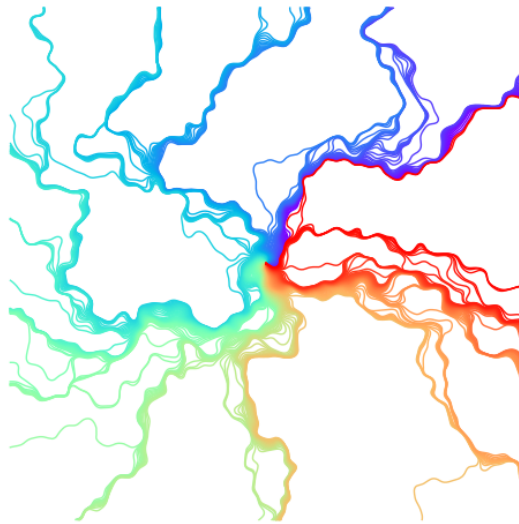
STAGE DE RECHERCHE

Quelques modèles de géométrie aléatoire

SLE, GFF et gravité quantique de Liouville

Chenlin GU

Ecole Polytechnique X2014



Option : Mathématiques appliquées

Champs de l'option : Modélisation probabilité et statistique

Directeur de l'option : Vincent BANSAYE

Directeur de stage : Pascal Maillard

Date du stage : 27/03/2017 - 28/07/2017

Nom de l'organisme : Université Paris-Sud

Déclaration d'intégrité relative au plagiat

Je soussigné GU Chenlin certifie sur l'honneur :

1. Que les résultats décrits dans ce rapport sont l'aboutissement de mon travail.
2. Que je suis l'auteur de ce rapport.
3. Que je n'ai pas utilisé des sources et des résultats tiers sans clairement les citer et les référencer selon les règles bibliographiques préconisées.

Je déclare que ce travail ne peut pas être suspecté de plagiat.

DATE : 1 Juillet 2017

Remerciements

J'aimerais tout d'abord remercier mon tuteur Pascal Maillard, qui encadre mon stage de recherche et me donne beaucoup d'opportunité et liberté d'explorer ce sujet. En plus, l'expérience de suivre son cours de processus branchant m'aide à passer dans la manière de travail plus académique et le cours est excellent.

Je tiens à remercier Grégory Miermont, Christophe Garban et les autres organisateurs de trimestre de probabilité à Lyon, où je passe deux semaines et rencontre beaucoup de chercheurs experts dans ce domaine (Marie Albenque, Marek Biskup, Timothy Budd, Jason Miller, Asaf Nachmias etc), qui accélère à apprendre des sujets.

Un merci à l'équipe de probabilité et statistique à Paris-Sud pour les activités académiques et les séminaires régulières. J'aimerais remercier aussi mes collègues de l'équipe EDP qui me offrent un bureau et partagent ses connaissances sur le transport optimal.

Finalement, je voudrais remercier CMAP pour me former une base solide avant mon aventure. En particulier, j'aimerais remercier à Igor Kortchemski et à Thierry Bodineau qui ouvrent la porte de géométrie aléatoire pour moi et m'encouragent toujours d'avancer.

Contents

1	Introduction	1
2	Schramm-Loewner evolution	3
2.1	Complex Loewner equation	4
2.1.1	Hydrodynamic mapping	5
2.1.2	Loewner flow	8
2.2	Chordal SLE	9
2.2.1	Conformal Markov property	9
2.2.2	Phases of SLE	11
3	Gaussian free field and Liouville quantum gravity	13
3.1	Discrete Gaussian free field	14
3.2	Definition and basic properties of GFF	16
3.2.1	GFF as white noise/ Gaussian process	17
3.2.2	GFF as a random distribution	17
3.2.3	Interpretation of GFF by path integral	19
3.3	Conformal invariance	20
3.4	Domain Markov property	21
3.5	Circle average	22
3.6	Construction of Liouville measure	27
3.7	γ -thick point	29
4	Gaussian multiplicative chaos theory	31
4.1	Basic frame	32
4.1.1	Comparison inequality	33
4.1.2	σ -positive kernel	33
4.1.3	Uniqueness	34
4.2	Non-degenerate limit measure	35
4.2.1	General situation	35
4.2.2	Case in \mathbb{R}^d	36
4.3	Further properties	37

4.4	Numerical experience : GFF and Liouville measure on $[0, 1]^2$	37
4.4.1	GFF on $[0, 1]^2$	37
4.4.2	Liouville measure on $[0, 1]^2$	38
4.4.3	Circle average	39
5	Imaginary geometry	41
5.1	Coupling of GFF and SLE	42
5.1.1	Why the flow should be a SLE ?	42
5.1.2	Theorem of coupling	43
5.2	Flow line, monotony, merging, crossing and light cone	47
5.2.1	Define a flow line by real method ?	49
5.3	Numerical experience : Flow line of GFF on unit disk	51
5.3.1	Choice of domain D	52
5.3.2	Simulation of GFF on any domain	52
6	Conclusion	55
A	Appendix	57
A.1	Riemann mapping theorem	57
A.2	Gaussian space and Gaussian process	58
A.3	Spectral of Laplace operator	59
A.4	Phase of Bessel process	60
B	Oberwolfach	62
B.1	Random geometry review	62
B.1.1	SLE	62
B.1.2	GFF/ γ -LQG	62
B.1.3	Random maps	63
B.1.4	SLE/GFF coupling	64
B.1.5	Quantum surface	65
B.1.6	Mating of trees	66
B.2	Open questions	66
B.2.1	Finding bijections	67
B.2.2	Gromov-Hausdorff vs Peanosphere vs Embedding convergence	67
B.2.3	Mismatch	67
B.2.4	String theory and Yang-Mills	67
B.2.5	Branching/Coalescence	67
B.2.6	Open question everyone knows	68
B.3	Personal thinking	68

List of Figures

1.1	Une simulation de quadrangulation planeaire	2
2.1	A simulation of $SLE_{8/3}$	3
2.2	A hydrodynamic mapping from $\mathbb{H} \setminus K \rightarrow \mathbb{H}$	5
2.3	An image to show the conromal Markov property - after being eaten one segment, the rest has the same distribution as the original one.	10
2.4	Phase diagram : From left to right is respectively $0 \leq \kappa \leq 4, 4 < \kappa < 8$ and $\kappa \leq 8$	12
3.1	A sample of GFF on the area $[0, 1]^2$. We take discretization of 200×200 and sum for $1 \leq j, k \leq 120$	13
3.2	The covariance between two circle average whose disks are disjoint.	25
3.3	Two methods to do double integration. The left one means we do integration over the big circle and the right one means we do integration over the small circle. However, if we start from the big circle, $G(x, y)$ is not harmonic in the disk and we cannot apply the mean value principle. So we prefer to do integration from the small one.	26
4.1	A sample of Liouville measure with parameter $\gamma = 0.5$	38
4.2	A sample of Liouville measure with parameter $\gamma = 1$	38
4.3	A sample of Liouville measure with parameter $\gamma = \sqrt{2}$	39
4.4	A sample of Liouville measure with parameter $\gamma \rightarrow 2$	39
4.5	A simulation of 1000 traces of $h_{e^{-t}}(0)$ for $t \in \{0, 0.1, 0.2 \dots 1.0\}$	40
5.1	Two flow lines of $\eta_{x_1}^{\theta_1}$ (yellow) and $\eta_{x_2}^{\theta_2}$ (red) where $x_1 \geq x_2, \theta_1 < \theta_2$. Then $\eta_{x_1}^{\theta_1}$ is always on the right hand side of $\eta_{x_2}^{\theta_2}$. They may meet each other, but once they meet, they will rebound instead of crossing.	48

5.2	Two flow lines of $\eta_{x_1}^{\theta_1}$ (yellow) and $\eta_{x_2}^{\theta_2}$ (red) where $x_1 \geq x_2, \theta_1 = \theta_2$. Then once $\eta_{x_1}^{\theta_1}$ and $\eta_{x_2}^{\theta_2}$ meet each other, they will merge and then evolve in a same trace.	48
5.3	Two flow lines of $\eta_{x_1}^{\theta_1}$ (yellow) and $\eta_{x_2}^{\theta_2}$ (red) where $x_1 \geq x_2, \theta_1 > \theta_2$. Then once $\eta_{x_1}^{\theta_1}$ and $\eta_{x_2}^{\theta_2}$ meet each other, one will cross the other. However, the crossing like that happens at most one time.	49
5.4	A simulation of flow lines starting from different point with a same angle. There will finally be a coalescence. If the angle is $\frac{\pi}{2}$, it's one branch of mating of trees.	50
5.5	A simulation of flow lines starting from one point with different angles represented by the colors.	50
5.6	A simulation of flow line from $-i$ to i on unit disk	51
5.7	A simulation of the harmonic extension on the unit disk	53
5.8	A simulation of a GFF on the unit disk by subtracting a harmonic extension from a GFF on the square $[-1, 1]^2$	53

1

Introduction

La géométrie aléatoire est un domaine très vivant et très riche, mais qu'est-ce que c'est la géométrie aléatoire ? Dans le dictionnaire de mathématiques, je crois qu'il y a une définition rigoureuse sur ce mot, mais il indique un objet aléatoire qui contient un peu plus de structure que juste un processus. Par exemple, le modèle de Galton-Watson est un processus aléatoire si l'on regarde le développement d'une famille, mais aussi un arbre aléatoire si l'on compare la généalogie entre plusieurs instances. Alors, tout dépend du point de vue.

En conséquence, la géométrie aléatoire n'est pas un domaine tout nouveau et cela existe depuis longtemps. Des modèles classiques comme le processus branchant, le graphe aléatoire, le modèle d'Ising et la percolation dans différents réseaux ont beaucoup développé dans la communauté de maths et aussi d'autres disciplines comme la physique, la biologie et l'informatique et sont beaucoup utilisés dans les modèles de populations, l'analyse de télécommunication et la finance etc. En particulier, l'invention de l'évolution de Schramm-Loewner, comme un événement marquant, donne une recette de décrire la limite de beaucoup d'objets aléatoires, puis elle sollicite énormément de recherche.

Cependant, si l'on révisait l'histoire de la théorie de mesure, elle a été construite en fait déjà dans une carte assez large car l'objet aléatoire peut être dans l'espace métrique et la théorie dans l'espace polonais est assez puissante et beaucoup développée. Donc, peut-être on se demande s'il y a des objets aléatoires plus "structurés" ?

La réponse est oui ! Parce que les physiciens ont quelques fois essayé d'utiliser des maths dans leurs manières afin de comprendre le monde. Par exemple, [Pol81] propose une idée de faire l'intégration par tous les chemins possible sur sphère. Cette analogie d'intégration stochastique apparaît naturelle pour les physiciens, mais pas évidente pour les mathématiciens. C'est vingt ans après, les mathématiciens

réalisent la construction dans dimension 2 par la limite de triangulation, quadragulation [LG⁺13], [M⁺13] ou par donner un densité aléatoire [DS11], et finalement, on espère de montrer que les deux manières réalisent le même objet, qui est un grand projet en cours [MS⁺16e], [MS15], [MS16c], [MS16c]. D'ailleurs, cet objet possède beaucoup de propriétés intéressants et d'autre modèle (marché aléatoire, modèle d'Ising, la percolation) sur cette surface aléatoire ouvert aussi la porte de mieux comprendre les modèles classiques.

Concernant mon stage de recherche, le but n'est pas aller tellement loin de comprendre toute l'histoire car la volume dépasse trop. Le premier but de stage est lecture des articles pour comprendre quelques objets fondamentales comme SLE et GFF, qui me permet d'approfondir dans le futur. La seconde but personnelle est réaliser des jolies images qui me a attiré il y longtemps.

Le rapport est organisé comme le suivant. Le première chapitre donne une rapide introduction de SLE et les propriétés plus élémentaires. Le deuxième chapitre est la partie principale qui collectionne beaucoup de résultat sur GFF, un brique utilisé de construire la surface aléatoire. Le troisième chapitre discute une manière de coupler les deux en regardant la trace de SLE comme un flot dans GFF, dont le comportement est exotique comparant le flot classique. Ce couplage est outil essentiel de beaucoup de recherche récente et nous permet de voir des jolies images.

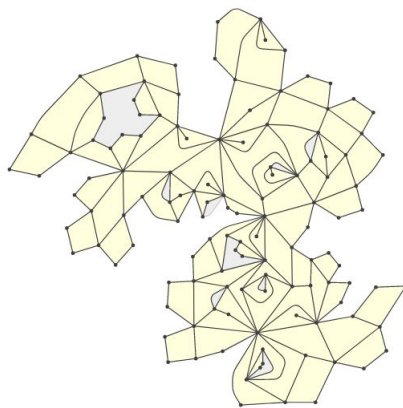


Figure 1.1: Une simulation de quadragulation planaire

2

Schramm-Loewner evolution

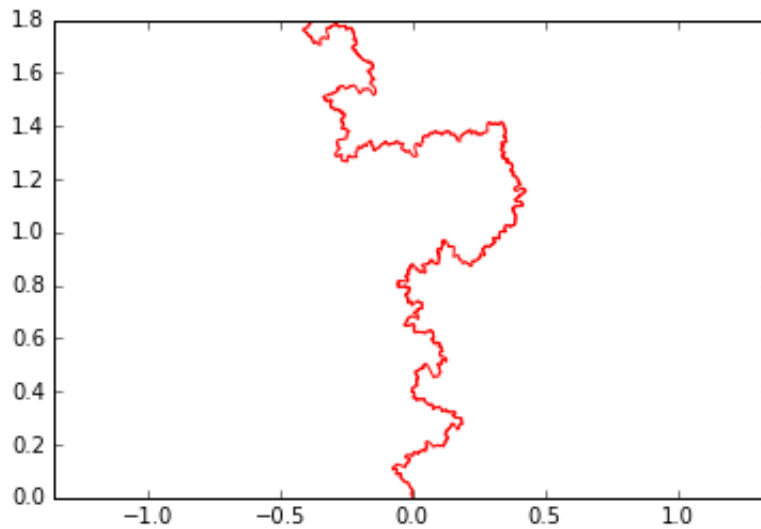


Figure 2.1: A simulation of $SLE_{8/3}$

Schramm-Loewner evolution may be one of the most interesting inventions in probability theory in last decades. It defines a conformal invariant random set generated by a trace, driven by a Brownian motion and the associated flow of conformal mapping. The behavior of the random set depends also on one parameter κ so we call always SLE_{κ} . This random object attracts people since it has been considered as the scaling limit of other discrete models when κ varies and some of them have been proved, i.e $\kappa = 2$ for loop erased random walk, $\kappa = 8$ for uniform spanning trees, $\kappa = 6$ for the interface of Ising model and $\kappa = 8/3$ for self-avoiding random walk etc.

Since this topic is so large and there is already a lot of excellent

references existing like [Wer04], [Law07], [Bef12], [RS11], this chapter aims at just a quick introduction of some basic notations and most necessary properties for the later chapter. This chapter is organized as following : the first section about complex Loewner introduces the some basic background knowledge in complex analysis, including some important estimations. Then we introduce the chordal SLE using the Loewner equation and we will prove that SLE is the only candidate of random local increment set satisfying conformal invariant property. The following part will introduce several properties such as its phase transition. Finally we remark that although the content of SLE is very rich, the beginner can treat it as a random process without regarding its connection with other models, which may lose some interests but get the idea and technique part of maths.

Reader can consult above references for further reading, especially the first one [Wer04] gives an overview and [Law07] as a comprehensive self-contained book. The master course notes accessible online of Jason Miller is also a good choice for master student. The three references above are also the base of this chapter. The method of simulation comes from the [Ken07].

2.1 Complex Loewner equation

In this chapter, we will recall some basic ideas from complex analysis and pave the way for define Loewner equation. In order to give an overview, we say something about SLE informally. SLE is a collection of conformal mapping $g_t : \mathbb{H} \setminus K_t \rightarrow \mathbb{H}$ where K_t is a family of compact subset in $\overline{\mathbb{H}}$ and $\mathbb{H} \setminus K_t$ is simply connected. g_t can be described as

$$\begin{aligned} \partial_t g_t(z) &= \frac{2}{g_t(z) - U_t} \\ g_0(z) &= z \end{aligned}$$

, where $U_t = \sqrt{\kappa}B_t$ and B_t is a standard Brownian motion. The set $\cup_{t \geq 0} K_t$ is generated by a curve from 0 to ∞ called the trace of SLE. A general SLE defined in a domain D connecting a and b is the image of conformal mapping $\phi : \mathbb{H} \rightarrow D, \phi(0) = a, \phi(\infty) = b$.

Some questions arise naturally : As Riemann mapping theory tells us, to fix the conformal mapping, we need at least one pair of corresponding points and the direction of derivative. Thus, how we could choose g_t ? Moreover, why we define the random set as above and does it has some special property ?

In this part, we will answer the first question about the choice of the conformal mapping g_t and its property is left to the next section.

2.1.1 Hydrodynamic mapping

We first introduce the concept of Hull, the object that we will study.

Definition 2.1.1 (Hull). $K \subset \bar{\mathbb{H}}$ is said a **Hull** if it is compact in $\bar{\mathbb{H}}$ and $\mathbb{H} \setminus K$ is simply connected in \mathbb{H} .

Then we need choose a good biconformal mapping $\mathbb{H} \setminus K \rightarrow \mathbb{H}$, because if ϕ is a biconformal mapping, then $a\phi + b, a, b \in \mathbb{R}$ is also one. In fact, the one we need is called **hydrodynamic mapping**.

Definition 2.1.2 (Hydrodynamic mapping). Given a Hull K , there exists a unique biconformal mapping $g_K : \mathbb{H} \setminus K \rightarrow \mathbb{H}$ such that

$$\lim_{z \rightarrow \infty} |g_K(z) - z| = 0.$$

If we develop the Laurent series of the mapping g_K at ∞ it has the form

$$g_K(z) = z + \frac{\text{hcap}(K)}{z} + \dots$$

where $\text{hcap}(K)$ is called the **capacity** of the K .

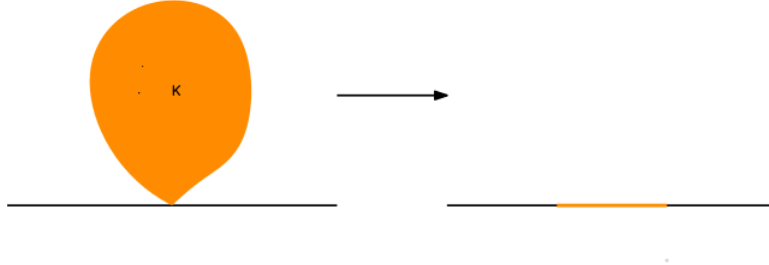


Figure 2.2: A hydrodynamic mapping from $\mathbb{H} \setminus K \rightarrow \mathbb{H}$

Proof. We prove at first the existence. The Riemann mapping theorem tells us the existence of a biconformal mapping $\tilde{g}_K : \mathbb{H} \setminus K \rightarrow \mathbb{H}$. We recall the Schwartz reflection lemma, which extends the mapping as $\tilde{g}_K(\bar{z}) = \overline{\tilde{g}_K(z)}$ so that we get a biconformal mapping

$$\tilde{g}_K : \mathbb{C} \setminus (K \cup \tilde{K}) \rightarrow \mathbb{C}.$$

Since $\lim_{z \rightarrow \infty} \tilde{g}_K(z) = \infty$ and $\tilde{g}'_K(0) \neq 0$, we construct a function $h_K(z) = 1/\tilde{g}(1/z)$ which is holomorphic and analytic at 0. Therefore,

$$h_K(z) = b_1 z + b_2 z^2 + b_3 z^3 \dots$$

where all the coefficients are real after the Schwartz reflection lemma. Comparing this formula with $\tilde{g}_K(1/z)$ we obtain

$$\begin{aligned}\tilde{g}_K(1/z) &= \frac{1}{b_1 z + b_2 z^2 + \dots} \\ \Rightarrow b_1 \tilde{g}_K(1/z) &= \frac{1}{z} \frac{1}{1 + \frac{b_2}{b_1} z + \dots} \\ &= \frac{1}{z} \left(1 - \frac{b_2}{b_1} z + cz^2 + \dots\right)\end{aligned}$$

Now we fix the scaling and translation of the biconformal mapping by setting $g_K(z) = b_1 \tilde{g}_K(z) + \frac{b_2}{b_1}$, then we develop the analytic series at ∞

$$g_K(z) = z + \frac{\text{hcap}(K)}{z} + \dots$$

Therefore we construct a biconformal mapping satisfying the condition.

We come to the proof of the uniqueness. Suppose that we have two biconformal mappings $g_K, \hat{g}_K : \mathbb{H} \setminus K \rightarrow \mathbb{H}$. Then $g_K \circ \hat{g}_K^{-1} : \mathbb{H} \rightarrow \mathbb{H}$ biconformal, so it has necessarily the structure

$$g_K \circ \hat{g}_K^{-1}(z) = \frac{az + b}{cz + d}, a, b, c, d \in \mathbb{R} \text{ and } ad - bc = 1$$

thanks to the theorem of Riemann mapping theorem. Moreover, the condition $\lim_{z \rightarrow \infty} |g_K(z) - z| = 0$ implies that

$$\lim_{z \rightarrow \infty} \frac{az + b}{cz + d} = \lim_{z \rightarrow \infty} g_K \circ \hat{g}_K^{-1}(z) = 1.$$

The only possible solution is that $a = d = 1$ and $b = c = 0$ which means $g_K = \hat{g}_K$ and this proves the uniqueness of the hydrodynamic mapping. □

The concept of $\text{hcap}(K)$ is very important since it measures the size of the Hull K . In the latter chapter, we will see that it is the parameter for the flow of hydrodynamic mapping, informally the capacity represents the time. To realize it, the capacity should be positive which is unknown for the instant. So, we will prove it and some useful propositions of the capacity.

Proposition 2.1.1. *Given K a Hull in \mathbb{H} , then its capacity satisfies the following properties*

1. **Positivity** : Given a Brownian motion and denote the hitting time $\tau = \inf\{t | B_t \notin \mathbb{H} \setminus K\}$, then

$$\text{hcap}(K) = \lim_{y \rightarrow +\infty} y \mathbb{E}_{iy}[\mathfrak{S}(B_\tau)].$$

2. **Scaling** : $\forall r > 0$

$$\text{hcap}(rK) = r^2 \text{hcap}(K).$$

3. **Invariance under translation** :

$$\text{hcap}(K + x) = \text{hcap}(K)$$

4. **Monotony** : Given $K \subset \tilde{K}$ two Hulls, then

$$\text{hcap}(\tilde{K}) = \text{hcap}(K) + \text{hcap}(g_K(\tilde{K} \setminus K)).$$

Proof. 1. Because the function $\mathfrak{S}(\cdot)$ is a harmonic function, the solution of Dirichlet problem can be represented as

$$\mathfrak{S}(z - g_K(z)) = \mathbb{E}_z[\mathfrak{S}(B_\tau - g_K(B_\tau))] = \mathbb{E}_z[\mathfrak{S}(B_\tau)]$$

We plug $z = iy$ into the formula

$$\begin{aligned} \lim_{y \rightarrow \infty} y \mathbb{E}_{iy}[\mathfrak{S}(B_\tau)] &= \lim_{y \rightarrow \infty} y \mathfrak{S}(iy - g_K(iy)) \\ &= \lim_{y \rightarrow \infty} y \mathfrak{S}\left(-\frac{\text{hcap}(K)}{iy} + o\left(\frac{1}{y}\right)\right) \\ &= \text{hcap}(K). \end{aligned}$$

As the capacity is the limit of probability, so it is necessarily positive.

2. $rg_K(x/r) : \mathbb{H} \setminus rK \rightarrow \mathbb{H}$ is a biconformal mapping satisfying

$$\begin{aligned} \lim_{z \rightarrow \infty} |rg_K(z/r) - z| &= \lim_{z \rightarrow \infty} \left| r\left(z/r + \frac{r \text{hcap}(K)}{z} + o\left(\frac{1}{z}\right)\right) - z \right| \\ &= \lim_{z \rightarrow \infty} \frac{r^2 \text{hcap}(K)}{z} + o(1) \\ &= 0. \end{aligned}$$

For the reason of uniqueness,

$$g_{rK}(\cdot) = rg_K(\cdot/r)$$

is the unique hydrodynamic mapping. From the calculus, we get that $\text{hcap}(rK) = r^2 \text{hcap}(K)$.

3. The proof is similar with the last one. We can check that

$$g_{K+x} = g_K(z - x) + x$$

and they have the same capacity.

4. We apply the uniqueness of hydrodynamic mapping and it's easy to check the following identity

$$g_{\tilde{K}} = g_{g(\tilde{K}\setminus K)} \circ g_K.$$

In fact, this equation says that we can eat the compact \tilde{K} in two steps : we use g_K to eat at first its subset K , and then apply another conformal application to eat the rest in the image. Then we calculate the capacity on the two sides

$$\begin{aligned} \text{hcap}(\tilde{K}) &= \lim_{z \rightarrow \infty} z(g_{g(\tilde{K}\setminus K)} \circ g_K(z) - z) \\ &= \lim_{z \rightarrow \infty} z \left(g_K(z) + \frac{\text{hcap}(g(\tilde{K}\setminus K))}{g_K(z)} + o\left(\frac{1}{g_K(z)}\right) - z \right) \\ &= \lim_{z \rightarrow \infty} z \left(z + \frac{\text{hcap}(K)}{z} + \frac{\text{hcap}(g(\tilde{K}\setminus K))}{z} + o\left(\frac{1}{z}\right) - z \right) \\ &= \text{hcap}(K) + \text{hcap}(g(\tilde{K}\setminus K)). \end{aligned}$$

It's the identity wanted. □

2.1.2 Loewner flow

The next step is to make the hydrodynamic mapping as a dynamic. Of course, this Hull should have some good property so that it could be described by equations.

Definition 2.1.3 ("Good" Hull). A family of Hull $\{K_t\}_{t \geq 0}$ is said "Good" if it satisfies the following properties :

1. **Non-decreasing** $\forall 0 \leq s < t < \infty, K_s \subset K_t$.
2. **Locally increasing** $\forall \epsilon > 0, \exists \delta > 0$ such that $\forall s \leq t \leq s + \delta$

$$\text{diam}(g_s(K_t \setminus K_s)) < \epsilon.$$

3. **Good parameterization** $\text{hcap}(K_t) = 2t$.

The following theorem states the existence of a Loewner flow which characterizes the growth of a family of good hull.

Theorem 2.1.1 (Existence of Loewner flow). *For a family of good Hull described as above, we denote $g_t = g_{K_t}$, then there exists a real-valued continuous function U_t called **driven function** such that*

$$\begin{aligned}\partial_t g_t(z) &= \frac{2}{g_t(z) - U_t} \\ g_0(z) &= z.\end{aligned}$$

Moreover, the point η_t satisfying $g_t(\eta_t) = U_t$ is the local increment point of K_t .

We neglects the proof of this part since it will use some fine complex analysis for estimating the continuity. We send the reader interested to the reference [Law08]. Finally, we remark that the reverse procedure is also possible : given a continuous function U_t , we can generate a family of good Hull and the technique used in this construction is called the reverse flow.

Remark. The Loewner flow in fact has a very long history in complex analysis, but the application in probability is very recent. In fact, its context could be very general for example the driven function could be a measure. Except the SLE theory, some variant version like QLE [MS15] is also developed later for studying the connection between the Brownian map and Liouville Quantum gravity.

2.2 Chordal SLE

Once we put the the driven function in complex Loewner equation as a standard Brownian $U_t = \sqrt{\kappa}B_t$, the Hull becomes a random set K_t and this is chordal SLE $_{\kappa}$. However, it's not clear why we have to design U_t a Brownian motion. In this section, we explain it by focusing on its conformal Markov property, which makes the Brownian motion the only candidate. Moreover, we will study the phase of chordal SLE when κ varies.

2.2.1 Conformal Markov property

The conformal Markov property can be seen as a 2D version of independent stationary increment property.

Definition 2.2.1 (Conformal Markov property). A random family of good Hull has the conformal Markov property if the following two conditions are satisfied

1. **Markov property** $\{g_t(K_{t+s}) - U_t\}_{s \geq 0}$ is independent with \mathcal{F}_t the filtration of the driven function, and it has the same law as $\{K_t\}_{t \geq 0}$.
2. **Scaling property** $\{\frac{1}{\sqrt{r}}K_{rt}\}_{t \geq 0}$ has the same law as $\{K_t\}_{t \geq 0}$.

One important reason to design a Brownian motion as a driven function is the following property.

Proposition 2.2.1 (Conformal Markov property). *Suppose that $\{K_t\}$ is the family of Hull defined by the flow of Loewner, it has conformal Markov property if and only if $U_t = \sqrt{\kappa}B_t$.*

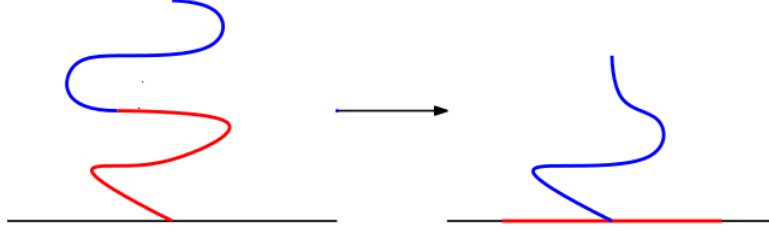


Figure 2.3: An image to show the conformal Markov property - after being eaten one segment, the rest has the same distribution as the original one.

Proof. We prove at first that the two property determine the driven function. The Loewner equation at time $t + s$ tells us

$$\frac{\partial}{\partial s}(g_{s+t}(z) - U_t) = \frac{2}{(g_{t+s}(z) - U_t) - (U_{t+s} - U_t)}.$$

Using the composition of Loewner flow we have

$$g_{t+s}(z) - U_t = g_{s,t} \circ g_t(z) - U_t = \tilde{g}_s(g_t(z) - U_t),$$

where \tilde{g}_s can be seen as a hydrodynamic mapping after g_t . This idea appears in last subsection. We substitute it in the equation

$$\frac{\partial}{\partial s} \tilde{g}_s(g_t(z) - U_t) = \frac{2}{\tilde{g}_s(g_t(z) - U_t) - (U_{t+s} - U_t)}$$

It generates a random set $g_t(K_{t+s}) - U_t$. We compare this equation with the equation of Loewner. It satisfies the Markov property if and only if

$U_{t+s} - U_t \stackrel{d}{=} U_s$ and independent with \mathcal{F}_t . That means U_t is a continuous process with stationary independent increment, so $U_t = aB_t + b$.

Moreover, the Loewner flow $\frac{1}{\sqrt{\lambda}}g_{\lambda t}(\sqrt{\lambda}\cdot)$ satisfies the equation

$$\frac{\partial}{\partial t} \frac{1}{\sqrt{\lambda}}g_{\lambda t}(\sqrt{\lambda}z) = \frac{2}{\frac{1}{\sqrt{\lambda}}g_{\lambda t}(\sqrt{\lambda}z) - \frac{1}{\sqrt{\lambda}}U_{\lambda t}}.$$

and this flow generate the random set $\frac{1}{\lambda}K_{\lambda t}$. It satisfies the scaling property if and only if $\frac{1}{\sqrt{\lambda}}U_{\lambda t} \stackrel{d}{=} U_t$. Combining the Markov property, the only candidate is that the driven function is a Brownian motion $U_t = \sqrt{\kappa}B_t$.

On the other hand, we put Brownian motion into the equation and check two identities above. It's not hard to find that the two two properties are met. \square

Remark. When we do scaling limit of some 2D discrete random objects, the limits usually have the conformal Markov property, i.e the loop erased random walk, so the only candidate should be SLE_{κ} . That's why SLE_{κ} plays a special role and the reason why the driven function is a Brownian motion.

One may wonder what happens if we put other driven function. Of course, we can put the other driven function in the equation and it has its own application in some case as a variant of SLE. We will see it in the later chapter.

2.2.2 Phases of SLE

Sometimes people abuse the usage of the word SLE to refer the curves or the Hulls or the Loewner flow. Sometimes they are indeed the same object but they may be different in other cases. To understand it, we need understand the phase of SLE .

Theorem 2.2.1 (Phase of SLE). *When $\kappa \leq 4$, almost surely $(\cup_{t \geq 0} K_t) \cap \mathbb{R} = \{0\}$ and K_t is a curve non self-intersecting.*

When $\kappa > 4$, almost surely $\mathbb{R} \subset (\cup_{t \geq 0} K_t)$ and K_t intersects itself.

Proof. The phase of SLE relates the behavior of Bessel process. We recall the d-dimensional Bessel is recurrent if and only if $0 < d < 2$. Concerning, SLE_{κ} , where we can find a Bessel process. $\forall z \in \mathbb{R}$ and we

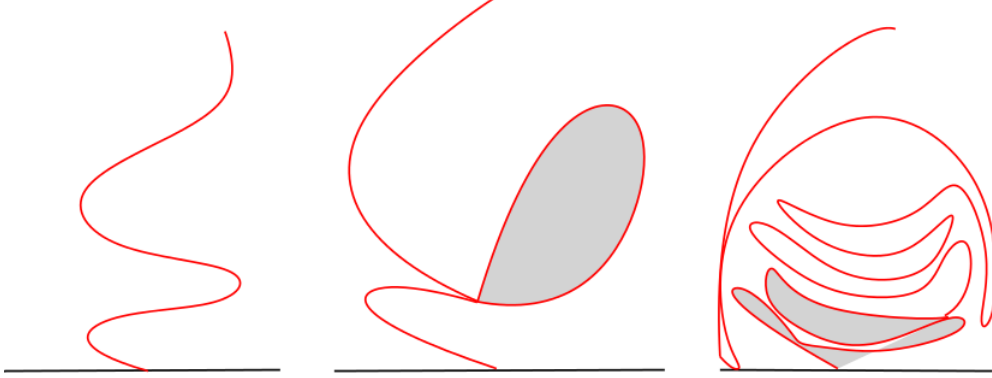


Figure 2.4: Phase diagram : From left to right is respectively $0 \leq \kappa \leq 4$, $4 < \kappa < 8$ and $\kappa \leq 8$.

denote $Y_t = g_t(z) - U_t$, then Y_t satisfies

$$\begin{aligned} dY_t &= \frac{2}{g_t(z) - U_t} dt - dU_t \\ &= \frac{2}{Y_t} dt + \sqrt{\kappa} dB_t \\ \Rightarrow dY_t/\sqrt{\kappa} &= \frac{2/\kappa}{Y_t/\sqrt{\kappa}} + dB_t. \end{aligned}$$

Therefore, $Y_t/\sqrt{\kappa}$ is a $(1 + \frac{4}{\kappa})$ Bessel process.

We interpret this result for SLE_κ . When $\kappa > 4 \Rightarrow d = 1 + \frac{4}{\kappa} < 2$ then the $Y_t/\sqrt{\kappa}$ is recurrent, so almost surely $\forall z \in \mathbb{R}$, $\exists t$ such that $g_t(z) = U_t$ which means $\mathbb{R} \subset \cup_{t \geq 0} K_t$. Conversely, when $\kappa \leq 4 \Rightarrow d \geq 2$, the Y_t will not touch 0 and z will not be eaten by the Hull K_t . Thus, $\cup_{t \geq 0} K_t \cap \mathbb{R} = \{0\}$.

Some further analysis reveals the surprising behavior of the curve K_t . As the Markov property tells us, $g_t(K_{t+s}) - U_t$ has the same law as K_s so almost surely it will not touch the real axis when $\kappa \leq 4$, which means the curve after time t will not touch the curve before time t since the image of the curve before time t is lying in the real axis. Thus, in this case the curve isn't self-intersecting. The same argument applies to the case $\kappa > 4$. □

Remark. When $\kappa \leq 4$ the SLE_κ is a simple curve and when $\kappa > 4$ it is generated by a simple curve. Moreover, when $\kappa \geq 8$ the curve generating SLE_κ is a space-filling. The precise description about the phase can be found in [RS11].

3

Gaussian free field and Liouville quantum gravity

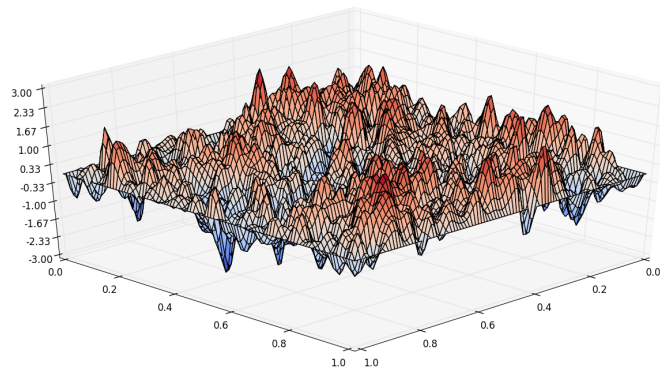


Figure 3.1: A sample of GFF on the area $[0, 1]^2$. We take discretization of 200×200 and sum for $1 \leq j, k \leq 120$

We know a Brownian motion can simulate a white noise in the nature, but how to describe a family of random noise on the surface? In this chapter we will study this question and study a new random object called Gaussian free field and its applications.

We will give at first the definition of Gaussian free field (GFF) introduced in [She07], a random distribution, which is a generalization of Brownian motion in \mathbb{R}^2 . The second part of this chapter is using GFF to construct Liouville quantum gravity (LQG), a concept coming from theoretical physics, defined as a random density as the exponential of Gaussian free field. The main task of the construction is how to make sense the definition in mathematics rigorously. Here, we remark that

the construction of LQG can be treated as a special case of a more general Gaussian multiplicative chaos theory developed in 80th by J.P Kahane, so we add one section to introduce this nice theory. Finally, we finish this chapter by various numerical experiences and visualizations.

The content about Gaussian free field in this chapter bases mainly on the [She07] and that about Liouville quantum gravity is based on [DS11] and [Gar12]. The part about Gaussian multiplicative chaos can be referred [Kah85] and recent review [RV⁺14]. Some part about discrete Gaussian free field comes from personal note in during the mini-school in Lyon. [Ber15] is also an excellent text book.

3.1 Discrete Gaussian free field

We start by defining a discrete Gaussian free field (DGFF) on subset of \mathbb{Z}^d as a Gaussian vector.

Definition 3.1.1 (Discrete Gaussian free field (DGFF)). Given $V \subset \mathbb{Z}^d$ finite. We define the discrete Gaussian free field a random vector $(h(x))_{x \in V}$ with the law

$$\mathbb{P}(h^V \in A) = \frac{1}{N} \int_A \exp\left(-\frac{1}{4d} \sum_{x \sim y} |h^V(x) - h^V(y)|^2\right) \Pi_{x \in V} dh^V(x)$$

where N is the constant of normalization.

We refer the language of analysis on graph and the $\mathbb{P}(h^V) \propto \exp -|\nabla h^V|^2$, which is related to the Boltzmann distribution of the Dirichlet energy if we see it as a statistical physics model. We can reduce the density to see the matrix of covariance, but we prefer to use the discrete Green function to study the correlation between different point.

Definition 3.1.2 (Discrete Green function). We define the discrete Green function by the simple random walk X_n on \mathbb{Z}^d .

$$G^V(x, y) = \mathbb{E}_x \left[\sum_{n=0}^{\tau-1} \mathbf{1}_{X_n=y} \right]$$

where $\tau = \inf\{n \geq 0, X_n \notin V\}$.

Proposition 3.1.1. 1. **Monotony** : $V \rightarrow G^V(x, y)$ is positive and non-decreasing.

2. **Symmetry** : $\forall x, y \in \mathbb{Z}^d, G(x, y) = G(y, x)$.

3. **Positive definite** : $\forall f \in \mathbb{Z}^d : \mathbb{R}, \text{supp}(f) < \infty$ we have

$$\sum_{x,y} f(x)f(y)G^V(x,y) \geq 0$$

4. **Fundamental solution** : $\forall x \in V, G^V(x,y)$ solves

$$\begin{aligned} -\Delta G^V(x, \cdot) &= \delta_x(\cdot) \text{ in } V \\ G^V(x, \cdot) &= 0 \text{ in } V^C \end{aligned}$$

where $-\Delta$ is a version of discrete Laplacian operator defined as

$$-\Delta f(x) = f(x) - \frac{1}{2d} \sum_{y \sim x} f(y)$$

Proof. 1. For two domain $V \subset \tilde{V}$, one can do coupling of two random walks so that they coincide before hitting the boundary, this gives automatically the monotony thanks to the definition of $G^V(x,y)$.

2. One important observation is that $G^V = (-\Delta)^{-1}$ where $(-\Delta) = Id - P$ and P is the transition matrix of the random walk. It suffices to check $(Id - P)G^V = Id$

$$\begin{aligned} \text{If } y \neq x, (Id - P)G^V(x,y) &= \sum_{x \sim z} (Id_{x \neq z} - P(x,z))G^V(z,y) \\ &= G^V(x,y) - \sum_{z \sim x} P(x,z)G^V(z,y) \\ &= G^V(x,y) - G^V(x,y) = 0 \end{aligned}$$

$$\begin{aligned} \text{If } y = x, (Id - P)G^V(x,y) &= G^V(x,x) - \sum_{z \sim x} P(x,z)G^V(z,x) \\ &= 1. \end{aligned}$$

Notice that P the simple random walk is reversible, so P is symmetry and so is $(Id - P)^{-1}$ and G^V .

3. Using the fact $G^V = (-\Delta)^{-1}$ and $(-\Delta)^{-1}$ is definite positive, so

$$\sum_{x \sim y} f(x)f(y)G^V(x,y) = \sum_{x \sim y} f(x)(Id - P)^{-1}f(y) \geq 0.$$

4. This property is contained in the proof of the first term. □

Once we have the definition of Green function, we obtain

Proposition 3.1.2. *Given $V \subset \mathbb{Z}^d$, $h^V = \mathcal{N}(0, G^V)$. That is to say the covariance between x and y is $G^V(x, y)$ i.e*

$$\text{Cov}(h(x), h(y)) = G^V(x, y).$$

Proof. It suffices to prove that

$$\exp\left(-\frac{1}{4d} \sum_{x \sim y} (h(x) - h(y))^2\right) = \exp\left(-\frac{1}{2} \langle h, (G^V)^{-1} h \rangle\right)$$

We do just calculus

$$\begin{aligned} \langle h, (G^V)^{-1} h \rangle &= \langle h, (Id - P)h \rangle \\ &= \sum_{x \sim y} h(x) \left(Id_{x=y} - \frac{1}{2d} \mathbf{1}_{x \sim y} \right) h(y) \\ &= \sum_x (h(x))^2 - \frac{1}{2d} \sum_{x \sim y} h(x) h(y) \\ &= \sum_x \sum_{y \sim x} \frac{1}{2d} \left[\frac{1}{2} (h(x) + h(y))^2 - h(x) h(y) \right] \\ &= \sum_x \sum_{y \sim x} \frac{1}{4d} (h(x) - h(y))^2 \\ &= \sum_{x \sim y} \frac{1}{2d} (h(x) - h(y))^2 \end{aligned}$$

Therefore h is a Gaussian vector with covariance G^V and of course we have $\text{Cov}(h(x), h(y)) = G^V(x, y)$. \square

3.2 Definition and basic properties of GFF

As the construction of Brownian motion, we have also many methods to define a GFF. But it lives as a random object in which space? In this section, we treat it from the view point of white noise, Gaussian process and a random distribution.

We suppose that the definition of distribution is well-known, otherwise the textbook of Ecole Polytechnique [Gol] is a good choice. Here, we just recall some properties of Soblev space.

Definition 3.2.1 (Dirichlet energy). $\forall D \subset \mathbb{R}^d, \forall f \in C_c^\infty(D)$, its Dirichlet energy is defined as

$$\|f\|_{\nabla}^2 = \frac{1}{2\pi} \int_D \nabla f(x) \cdot \nabla f(x) dx$$

this induces a scalar product $\langle \cdot, \cdot \rangle_{\nabla}$ and the completion of $C_c^\infty(D)$ under this norm is noted $H_0^1(D)$ as Soblev space of Dirichlet boundary.

3. GAUSSIAN FREE FIELD AND LIOUVILLE QUANTUM GRAVITY 17

We restrict us in the case \mathbb{R}^2 except further explanation. Under this context, the product is invariant under scaling $f_\lambda(\cdot) = f(\lambda \cdot)$.

3.2.1 GFF as white noise/ Gaussian process

The most natural way to treat GFF is from the view point of Gaussian process and white noise. We reader can find the basic definition in appendix.

Definition 3.2.2 (GFF as white noise). Given $D \subset \mathbb{R}^2$ and a Hilbert space $H_0^1(D)$, GFF h is defined as a white noise on $H_0^1(D)$ i.e an isometry between $H_0^1(D)$ and a Gaussian space.

That is to say, $\forall f, g \in H_0^1(D)$, $h(f) \sim \mathcal{N}(0, \|f\|_\lambda^2)$ and

$$\mathbb{E}[h(f)h(g)] = \int_D \nabla f(x) \cdot \nabla g(x) dx$$

Since a white noise can be also treated as Gaussian process indexed by function, we give the definition of GFF as a Gaussian process.

Definition 3.2.3 (GFF as Gaussian process). A GFF h defined on D is a Gaussian process $\{h(f)\}_{f \in H_0^1(D)}$ indexed by function in $H_0^1(D)$, whose covariance matrix is

$$K(f, g) = \mathbb{E}[h(f)h(g)] = \langle f, g \rangle_\nabla$$

3.2.2 GFF as a random distribution

As mentioned in the appendix, we have canonical construction of a white noise by the orthogonal normal basis. Here, we give the definition and we will prove that, by this canonical construction, h lives in $H_0^{-1}(D)$ as a random distribution(In the sense of Schwartz distribution).

Definition 3.2.4 (Gaussian free field as a random distribution). Given $\{e_i\}_{i \geq 1}$ a family of orthonormal basis of $H_0^1(D)$, then the Gaussian free field h is defined as a random distribution

$$h = \sum_{i=1}^{\infty} X_i e_i$$

where $\{X_i\}_{i \geq 1}$ is a family of independent random variable of law $\mathcal{N}(0, 1)$.

A first question is whether this object is well defined and does this definition depend on the choice of the basis? Although the range of distribution is large enough, an infinite sum risks making the functional too "large". The following proposition shows that this definition makes sense in distribution.

Proposition 3.2.1. 1. $\forall f \in H_0^1(D), \langle h, f \rangle_{\nabla} \sim \mathcal{N}(0, \|f\|_{\nabla}^2)$.

2. Further more, $\forall f, g \in H_0^1(D)$ we can also calculate the covariance between $\langle h, f \rangle_{\nabla}, \langle h, g \rangle_{\nabla}$,

$$\text{Cov}(\langle h, f \rangle_{\nabla}, \langle h, g \rangle_{\nabla}) = \langle f, g \rangle_{\nabla}$$

3. Finally, almost surely, the GFF is a random object valued in $H_0^{-1}(D)$.

Proof. 1. Suppose that $f = \sum_{i=1}^{\infty} \alpha_i e_i$ then the Dirichlet product is

$$\langle h, f \rangle_{\nabla} = \sum_{i=1}^{\infty} \alpha_i X_i$$

who is a sum of infinite independent Gaussian. Due to the property of Gaussian vector, it's itself a Gaussian with mean 0 and variance

$$\text{Var}(\langle h, f \rangle_{\nabla}) = \mathbb{E} [\langle h, f \rangle_{\nabla}^2] = \sum_{i=1}^{\infty} \alpha_i^2$$

and this coincides with the Dirichlet energy of f . This implies that almost surely, $\langle h, f \rangle_{\nabla}$ is finite. Moreover, this also shows that the definition of GFF doesn't depend on the choice of the basis.

2. The calculus of covariance is no harder. Given $g = \sum_{j=1}^{\infty} \beta_j X_j$,

$$\text{Cov}(\langle h, f \rangle_{\nabla}, \langle h, g \rangle_{\nabla}) = \mathbb{E} \left[\sum_{i=1}^{\infty} \alpha_i X_i \sum_{j=1}^{\infty} \beta_j X_j \right] = \sum_{i=1}^{\infty} \alpha_i \beta_i$$

and it's the answer of $\langle h, g \rangle_{\nabla}$.

3. We can prove even stronger version of this theorem that h lives in the space $H_0^{-\epsilon}(D), \epsilon > 0$. The Soblev space with negative index $-s$ is defined as the dual space of the index s . Here, we will use an equivalent definition defined by a very specific orthogonal normal basis. Reader can check [A.3](#) for the relevant definition and theorem.

We pick the L^2 orthogonal normal basis $\{l_n\}_{n \geq 1}$ of $(-\Delta)^{-1}$, then it is easy to check that $\{\frac{1}{\sqrt{\lambda_n}} l_n\}_{n \geq 1}$ forms an orthogonal normal basis of $H_0^1(D)$. Then a canonical construction of GFF by this basis is

$$h = \sum_{n=1}^{\infty} \frac{X_n}{\sqrt{\lambda_n}} l_n$$

3. GAUSSIAN FREE FIELD AND LIOUVILLE QUANTUM GRAVITY 19

where $\{X_n\}_{n \geq 1}$ are i.i.d Gaussian. Then we calculate is expectation of $H_0^{-\epsilon}(D)$ norm

$$\begin{aligned} \|h\|_{H_0^{-\epsilon}}^2 &= \sum_{n=1}^{\infty} \left(\frac{X_n}{\sqrt{\lambda_n}} \right)^2 (\lambda_n)^{-\epsilon} = \sum_{n=1}^{\infty} \frac{(X_n)^2}{\lambda_n^{1+\epsilon}} \\ \mathbb{E}[\|h\|_{H_0^{-\epsilon}}^2] &= \sum_{n=1}^{\infty} \frac{1}{\lambda_n^{1+\epsilon}} \asymp \sum_{n=1}^{\infty} \frac{1}{n^{1+\epsilon}} < \infty \end{aligned}$$

In the last line, we use the theorem of Weyl. This implies that almost surely $\|h\|_{H_0^{-\epsilon}(D)}^2 < \infty$, so it is a random distribution. \square

3.2.3 Interpretation of GFF by path integral

This part is taken from the lecture notes by Vincent Vargas at IHES. Treating GFF as a random Schwartz distribution, one can interpret the GFF as the path integral in physics.

Physicists study the path integral

$$\int_{L(\mathbb{S}^2)} F(\phi) e^{-\frac{1}{4\pi} \int_{\mathbb{C}} |\nabla \phi|^2 g(x) dx} D(\phi)$$

where $D(\phi)$ means a measure on all the $L(\mathbb{S}^2)$ function and $F(\phi)$ is a function of ϕ , λ is defined on sphere and $g(x)$ is the density function on sphere. It looks like an expectation of a random variable, except the definition of $D(\phi)$ is not so clear.

One method to treat this expectation is to treat it as the integration of Lebesgue on every projection of orthogonal basis. More precisely, we choose the eigenvectors $\{l_j\}_{j \geq 0}$ of Laplace as the orthogonal normal basis so

$$\phi = c + \sum_{j \geq 1} c_j l_j$$

and do Lebesgue integration on $c, \{c_j\}_{j \geq 1}$ then the integral becomes

$$\int_{\mathbb{R}} \int_{\mathbb{R}^{\mathbb{N}^*}} F(c + \sum_{j \geq 1} c_j l_j) dc \Pi_{j \geq 1} (e^{-\frac{c_j^2 \lambda_j}{4\pi}} dc_j)$$

.Finally, we apply the change of variable $u_j = c_j \sqrt{\lambda_j} / \sqrt{2\pi}$, we get

$$C \int_{\mathbb{R}} \int_{\mathbb{R}^{\mathbb{N}^*}} F(c + \sqrt{2\pi} \sum_{j \geq 1} u_j \frac{l_j}{\sqrt{\lambda_j}}) dc \Pi_{j \geq 1} (e^{-\frac{u_j^2}{2}} du_j)$$

. Since $\sqrt{2\pi} \sum_{j \geq 1} u_j \frac{l_j}{\sqrt{\lambda_j}} \xrightarrow{H^{-\epsilon}} h$ where the u_j is i.i.d Gaussian, formally, we write the path integral as

$$\int_{L(\mathbb{S}^2)} F(\phi) e^{-\frac{1}{4\pi} \int_{\mathbb{C}} |\nabla \phi|^2 g(x) dx} D(\phi) = \int_{\mathbb{R}} \mathbb{E}[F(h + c)] dc$$

. We remark that in the right hand side, the expectation and integration is in value of Schwartz distribution. Although h lives in the space of Schwartz distribution, $F(h + c)$ may not necessarily be the case especially in nonlinear case. Thus, in concrete situation, we should also make sense of it at first.

3.3 Conformal invariance

A first important property is that GFF is invariant under conformal mapping.

Proposition 3.3.1 (Conformal invariance). *Given $\phi : D \rightarrow \tilde{D}$ a conformal mapping and h a GFF on D , then $h \circ \phi^{-1}$ defines a GFF on \tilde{D} .*

Proof. Suppose that $\{e_i\}$ is an orthonormal basis in D , one important observation is that $\{e_i \circ \phi^{-1}\}$ is an orthonormal basis in \tilde{D} . In fact, the conformal mapping ϕ induces an isometry between $H_0^1(D)$ and $H_0^1(\tilde{D})$. We will prove this fact at first.

Denoting $(u, v) = \phi(x, y)$ and using the Cauchy-Riemann equation

$$\begin{cases} \frac{\partial u}{\partial x} = \frac{\partial v}{\partial y} \\ \frac{\partial u}{\partial y} = -\frac{\partial v}{\partial x} \end{cases}$$

, suppose that $f \in H_0^1(\tilde{D})$ and we calculate its norm by the change of variable and the equation above

$$\begin{aligned} \|f \circ \phi\|_{\nabla(\tilde{D})}^2 &= \int_D |\nabla(f \circ \phi)(x, y)|^2 dx dy \\ &= \int_D \left(\frac{\partial(u, v)}{\partial(x, y)} \cdot \nabla f(u, v) \right)^\top \left(\frac{\partial(u, v)}{\partial(x, y)} \cdot \nabla f(u, v) \right) dx dy \\ &= \int_D |\nabla f(u, v)|^2 \det \left(\frac{\partial(u, v)}{\partial(x, y)} \right) dx dy \\ &= \int_{\tilde{D}} |\nabla f(u, v)|^2 du dv = \|f\|_{\nabla(D)}^2 \end{aligned}$$

So $h \circ \phi^{-1} = \sum_{i=1}^{\infty} X_i e_i \circ \phi^{-1}$ is the sum of orthonormal basis of \tilde{D} with random i.i.d reduced centered Gaussian and so is GFF on \tilde{D} . \square

3.4 Domain Markov property

Unlike the DGFF, GFF is a distribution which makes it sometimes a little difficult to describe. In this section and the next section, we try to catch some other properties of GFF. This section we talk about its Markov domain property, a analogue property of the stationary increment property of Brownian motion.

Since the property of distribution always come back to the test function, we recall the proposition of orthogonal decomposition of $H_0^1(D)$ at first.

Proposition 3.4.1 (Orthogonal decomposition of $H_0^1(D)$). $\forall U \subset D$, $H_0^1(D)$ we have the following direct sum

$$H_0^1(D) = H_0^1(U) \oplus H_{Harm}(U)$$

where $H_{Harm}(U) \subset H_0^1(D)$ represents the subspace of harmonic function on U .

Proof. We know that $H_0^1(U)$ is the subspace of $H_0^1(D)$ and the orthogonal decomposition of Hilbert space tells us

$$H_0^1(D) = H_0^1(U) \oplus (H_0^1(U))^\perp$$

so what we need to do is to show that $(H_0^1(U))^\perp = H_{Harm}(U)$. The key formula to prove it is the integration by part : $\forall f, g \in C_c^\infty(D)$

$$\langle f, g \rangle_\nabla = \langle f, -\Delta g \rangle.$$

We suppose that $g \in H_{Harm}(U)$, then $\forall f \in H_0^1(U)$, the inner product of Dirichlet is 0 and this implies that $H_{Harm}(U) \subset (H_0^1(U))^\perp$.

On the other hand, if $g \in (H_0^1(U))^\perp$, then $\forall f \in H_0^1(U)$, $\langle f, g \rangle_\nabla = 0$ and the integration by part shows that $\Delta g = 0$ in the weak sense. Due to the regularity of elliptical operator, g is a harmonic function in strong sense. \square

The orthogonal decomposition of test function introduces the same structure on the distribution, namely a GFF can be written as the sum of a GFF support on sub-domain $U \in D$ and a harmonic function on it.

Theorem 3.4.1 (Orthogonal decomposition of GFF). $\forall U \subset D$, a GFF on D can be decomposed as

$$h = h_U + h_{Harm}$$

where h_U is a GFF on U and h_{Harm} is its conformal extension, so h_{Harm} is harmonic on U .

Proof. As what we do for the proof of the orthogonal decomposition of $H_0^1(D)$, we do projection of h on the orthonormal basis of $H_0^1(U)$ and we obtain a GFF h_U . It suffices to prove that $h - h_U$ is a harmonic function on U . We do the inner product of Dirichlet with a function $f \in C_c^\infty(U)$

$$\langle h - h_U, f \rangle_\nabla = 0$$

We use the integration by part formula and this means $h - h_U$ is harmonic in weak sense. Once again we recall the regularity of elliptical operator, so $h - h_U$ is a random harmonic function on U . \square

Remark. One may draw the analogue between the Markov property of Brownian motion and the Markov domain of GFF. This is possible, for Brownian motion and $0 < t < s$,

$$\mathbb{E}[B_s | \mathcal{F}_t] = B_t$$

, however, here informally we write

$$\mathbb{E}[h_D | \sigma(U^C)] = h_U + h_{Harm}$$

. Here, we use $\sigma(U^C)$ to represents all the information outside of the U , namely the σ -algebra generated by the random variable $h(f)$ where the support of function is outside of U . We refer [Aru15] for detailed discussion about the σ -algebra generated by domain.

This theorem tells that the information of GFF is hidden in the domain and sometimes we write its σ -algebra as $\sigma(U)$. A simple corollary is the following.

Corollary 3.4.1. *Let h be a GFF on domain D and $U_1, U_2 \in D, U_1 \cap U_2 = \emptyset$. Then the restrictions on these domains h_{U_1}, h_{U_2} are independent.*

One can prove this simple corollary by checking all the definition.

3.5 Circle average

Approximating a distribution by convolution is a classical strategy of distribution theory. For GFF we have a similar technique called circle average and we will study it in this section. Generally speaking, it's 'integration' of a GFF on a circle.

However, we have to explain what does 'integration' mean. If we take the integration by part technique, for two function $f, g \in C_c^\infty(D)$, we have

$$\langle f, g \rangle = \langle f, (-\Delta)(-\Delta)^{-1}g \rangle = 2\pi \langle f, (-\Delta)^{-1}g \rangle_\nabla$$

3. GAUSSIAN FREE FIELD AND LIOUVILLE QUANTUM GRAVITY 23

where the $(-\Delta)^{-1}g(x)$ is realized as the integration by a Green function. We recall the definition of the Green function. It satisfies

$$\begin{aligned}\frac{1}{2\pi}(-\Delta)G(x, \cdot) &= \delta_x(\cdot) \\ G(x, \cdot)|_{\partial D} &= 0\end{aligned}$$

and its value is given by

$$G(x, y) = -\log|y - x| - \tilde{G}(x, y)$$

where $\tilde{G}(x, y)$ is the harmonic function with boundary value

$$\tilde{G}(x, y)|_{\partial D} = -\log|y - x|.$$

The Dirichlet problem can be solved with the help of the Green function. The most important property is that

$$2\pi(-\Delta)^{-1}f(x) = \int_D G(x, y)f(y)dy$$

So we define the inner product of L^2 with GFF similarly.

Definition 3.5.1 (L^2 inner product of GFF). Given $D \subset \mathbb{R}^2$ and h a GFF on D , we define the product with a function f whose $(-\Delta)^{-1}g \in H_0^1(D)$ as

$$\langle h, f \rangle = \langle h, 2\pi(-\Delta)^{-1}f \rangle_{\nabla}$$

where the inverse of Laplacian is defined as an integration with the Green function

$$(-\Delta)^{-1}f(x) = \frac{1}{2\pi} \int_D G(x, y)f(y)dy.$$

The L^2 inner product gives also a Gaussian random variable whose law is described by the following proposition.

Proposition 3.5.1. $\forall f$ such that $(-\Delta)^{-1}f \in H_0^1(D)$, $\langle h, f \rangle$ is a Gaussian whose mean is zero and variance is $\langle 2\pi(-\Delta)^{-1}f, 2\pi(-\Delta)^{-1}f \rangle_{\nabla}$

$$\text{Var}(\langle h, f \rangle) = \int_{D \times D} f(x)G(x, y)f(y)dxdy$$

Moreover, $\forall f, g$ such that $(-\Delta)^{-1}f, (-\Delta)^{-1}g \in H_0^1(D)$ we can also calculate the covariance between $\langle h, f \rangle, \langle h, g \rangle$,

$$\text{Cov}(\langle h, f \rangle, \langle h, g \rangle) = \int_{D \times D} f(x)G(x, y)g(y)dxdy$$

3. GAUSSIAN FREE FIELD AND LIOUVILLE QUANTUM GRAVITY 24

Proof. From the definition, we see that the L^2 inner product is finally induced by the inner product of Dirichlet so it is a Gaussian with zero mean. We just calculate the covariance formula

$$\begin{aligned}
 \text{Cov}(\langle h, f \rangle, \langle h, g \rangle) &= \text{Cov}(\langle h, 2\pi(-\Delta)^{-1}f \rangle_{\nabla}, \langle h, 2\pi(-\Delta)g \rangle_{\nabla}) \\
 &= \langle 2\pi(-\Delta)^{-1}f, 2\pi(-\Delta)^{-1}g \rangle_{\nabla} \\
 &= \frac{1}{2\pi} \int_D (\nabla 2\pi(-\Delta)^{-1}f)(x) \cdot (\nabla 2\pi(-\Delta)^{-1}g)(x) dx \\
 &= 2\pi \int_D f(x)(-\Delta^{-1}g)(x) dx \\
 &= \int_{D \times D} f(x)G(x, y)g(y) dx dy
 \end{aligned}$$

□

We can check the L^2 product with a uniform measure of circle $\partial B_r(z)$ is well defined.

Definition 3.5.2 (Circle average). Given ρ_ϵ^z the uniform measure on $\partial B_\epsilon(z)$, we define the circle average of a GFF h on it as

$$h_\epsilon(z) = \langle h, \rho_\epsilon^z \rangle$$

.

Remark. One may be puzzled why we can put in the L^2 structure a measure. In fact, from the definition what we need check is

$$\langle 2\pi(-\Delta)^{-1}\rho_\epsilon^z, 2\pi(-\Delta)^{-1}\rho_\epsilon^z \rangle_{\nabla} = \int_D \rho_\epsilon^z(x)G(x, y)\rho_\epsilon^z(y) dx dy < \infty$$

. We will see that its value is $-\log(\epsilon) - \tilde{G}(z, z)$ in the following part, since the proof of proposition of circle is just a similar type of calculus.

The circle average of GFF gives a function, so it's easier to treat. One first proposition shows the connection between the GFF and DGFF, which says that when the two disks of circle are disjoint, then the circle average has a covariance of Green function.

Proposition 3.5.2. *If $B_{\epsilon_1}(z_1)$ and $B_{\epsilon_2}(z_2)$ are two disjoint disks i.e $|z_1 - z_2| > \epsilon_1 + \epsilon_2$, then*

$$\text{Cov}(h_{\epsilon_1}(z_1), h_{\epsilon_2}(z_2)) = G(z_1, z_2)$$

.

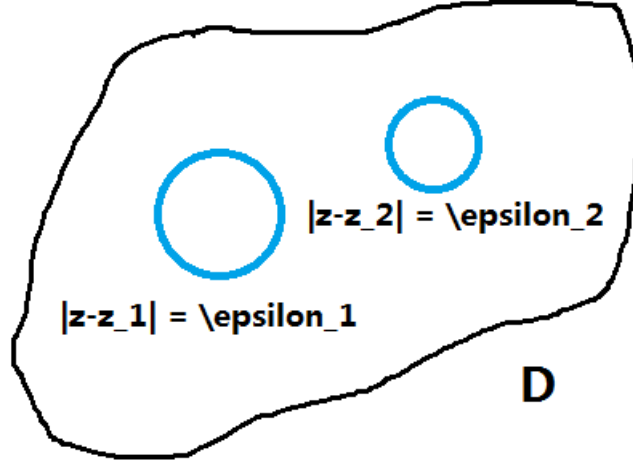


Figure 3.2: The covariance between two circle average whose disks are disjoint.

Proof.

$$\begin{aligned} \text{Cov}(h_{\epsilon_1}(z_1), h_{\epsilon_2}(z_2)) &= \int_{D \times D} \rho_{\epsilon_1}^{z_1}(x) G(x, y) \rho_{\epsilon_2}^{z_2}(y) dx dy \\ &= \frac{1}{2\pi} \int_{|z-z_1|=\epsilon_1} \frac{1}{2\pi} \int_{|z-z_2|=\epsilon_2} G(x, y) dx dy \end{aligned}$$

The case that two disks are disjoint assures that $B_{\epsilon_1}(z_1) \cap B_{\epsilon_2}(z_2) = \emptyset$, so that in the integration $x \notin \overline{B_{\epsilon_1}(z_1)}$, $y \notin \overline{B_{\epsilon_2}(z_2)}$ and $G(x, y)$ is always harmonic. Using the principle of mean value, we get that

$$\frac{1}{2\pi} \int_{|z-z_1|=\epsilon_1} \frac{1}{2\pi} \int_{|z-z_2|=\epsilon_2} G(x, y) dx dy = G(z_1, z_2).$$

□

The following theorem is the heart of the GFF and the base of the construction of Liouville measure. It studies the behavior of the circle average when varying the radius ϵ but fixing the center z .

Theorem 3.5.1 (Circle average is a Brownian motion). $h_{e^{-t}}(z)$ is a Brownian motion.

Proof. It suffices to calculate the covariance between $h_{e^{-t}}(z), h_{e^{-s}}(z), s < t$. We use the double integration of the proposition above

$$\text{Cov}(h_{e^{-t}}(z), h_{e^{-s}}(z)) = \frac{1}{2\pi} \int_{|x-z|=e^{-s}} \frac{1}{2\pi} \int_{|y-z|=e^{-t}} G(x, y) dx dy$$

3. GAUSSIAN FREE FIELD AND LIOUVILLE QUANTUM GRAVITY 26

However, there is some delicate technique in the order of integration. In order to apply the mean value principle, $G(x, y)$ have to be harmonic in the domain which means $x \neq y$. So, we prefer to do integration over the little circle. We remark that integration at first over the big circle is also possible but it requires more effort. In the second step, we have no choice but plug the expression of $G(x, y)$ into the formula.

Hence,

$$\begin{aligned} \text{Cov}(h_{e^{-t}}(z), h_{e^{-s}}(z)) &= \frac{1}{2\pi} \int_{|x-z|=e^{-s}} \frac{1}{2\pi} \int_{|y-z|=e^{-t}} G(x, y) dx dy \\ &= \frac{1}{2\pi} \int_{|x-z|=e^{-s}} G(x, z) dx \\ &= \frac{1}{2\pi} \int_{|x-z|=e^{-s}} -\log|x-z| - \tilde{G}(x, z) dx \\ &= s - \tilde{G}(z, z) \end{aligned}$$

Therefore, we obtain the result wanted.

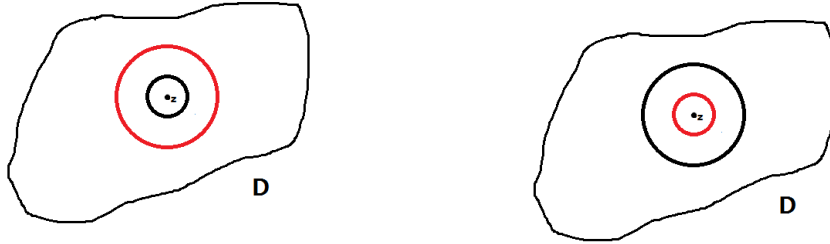


Figure 3.3: Two methods to do double integration. The left one means we do integration over the big circle and the right one means we do integration over the small circle. However, if we start from the big circle, $G(x, y)$ is not harmonic in the disk and we cannot apply the mean value principle. So we prefer to do integration from the small one.

□

Remark. The value of $-\tilde{G}(z, z)$ is of order $\text{dist}(z, \partial D)$ and is denoted $R(z, D)$. So we have

$$\text{Cov}(h_{e^{-t}}(z), h_{e^{-s}}(z)) = s \wedge t + R(z, D)$$

$R(z, D)$ is called conformal radius and it makes sense in the further application of local set.

3.6 Construction of Liouville measure

The role of GFF for 2D random object is the counterpart or Brownian motion for random process. However, since GFF is itself a random distribution, the definition of these 2D random objects is sometimes not so direct. In this section, we would like make sense of the exponential of random measure

$$e^{\gamma h} dz$$

which is defined as 2D Liouville quantum gravity.

Theorem 3.6.1 (Liouville measure). $\forall \gamma \in [0, 2)$, we define a family of random measure

$$\mu_\epsilon(dz) = e^{\gamma h_\epsilon(z)} \epsilon^{\gamma^2/2} dz$$

Then there exists a convergent sub-sequence which converges almost surely to a limit in a weak sense and we denote its limit as the Liouville measure $\mu(dz)$, i.e $\forall f \in C_c^\infty(D)$

$$a.s \mu_\epsilon(f) \xrightarrow{\epsilon \rightarrow 0} \mu(f)$$

.

Remark. Here we say the random measure converges in weak sense means we see μ_ϵ random object valued of measure on D as a member of Schwartz distribution. Then the weak convergence refers to the convergence of Schwartz distribution. However, in fact we can prove the proof of measure is almost surely U.I, so the limit is a true measure.

Remark. The Gaussian multiplicative chaos theory provides a more general frame to treat the convergence of random measure.

Before proving this theorem, we give some general description about this theorem and the frame of the proof.

At first, we have to understand what is a random measure. Informally, a random measure means that we sample a GFF instance h and then define a measure as above by circle average. For each point, the density is in fact a random variable so the measure for a Borel set $A \subset D$, denoted by $\mu_\epsilon^\gamma(A)$ is also a random variable. Moreover, $\mu_\epsilon^\gamma(dz)$ is a martingale with respect of the filtration $\sigma(B_r(z))$ since

$$\mu_\epsilon^\gamma(dz) = e^{\gamma h_\epsilon(z)} \epsilon^{\gamma^2/2} dz = e^{\gamma h_\epsilon(z) - \frac{1}{2} \text{Var}(h_\epsilon(z)) + \gamma^2/2 \log R(z,D)} dz$$

is the standard martingale of geometric Brownian motion. We know a positive martingale converge a.s to a limit martingale. However, it isn't sufficient since it may be degenerated. So we have to give some

3. GAUSSIAN FREE FIELD AND LIOUVILLE QUANTUM GRAVITY 28

estimation of convergence more precise to show that the limit is a measure.

We will treat only the easy part of the case $\gamma \leq \sqrt{2}$ and the difficult part $\sqrt{2} < \gamma < 2$ is left for the reference [B⁺17].

Proof. We will prove that there is a sub-sequence of random measure μ_ϵ^γ that converges in L^2 to its limit. Firstly, for any compact set $A \subset D$ and $B_\epsilon(A) \subset D$, $\mu_\epsilon^\gamma(A)$ is a random variable whose expectation is constant.

$$\begin{aligned} \mathbb{E}[\mu_\epsilon^\gamma(A)] &= \mathbb{E}\left[\int_A e^{\gamma h_\epsilon(z)} \epsilon^{\gamma^2/2}\right] \\ &= \int_A \mathbb{E}[e^{\gamma h_\epsilon(z)} \epsilon^{\gamma^2/2}] dz \\ &= \int_A (R(z, D))^{\gamma^2/2} dz \end{aligned}$$

Then, we prove that $\mu_{\frac{\epsilon}{2^k}}^\gamma(A)$ is a Cauchy sequence in L^2 . Observing that $h_\epsilon(z)$ is a Brownian motion, then the independent increment tells us

$$h_{2\epsilon} - h_\epsilon \perp h_\epsilon.$$

We use this property in the estimation of $\mathbb{E}[|\mu_{2\epsilon}^\gamma(A) - \mu_\epsilon^\gamma(A)|^2]$

$$\begin{aligned} &\mathbb{E}[|\mu_{2\epsilon}^\gamma(A) - \mu_\epsilon^\gamma(A)|^2] \\ &= \int_{A \times A} \mathbb{E}\left[(e^{\gamma h_{2\epsilon}(x)} (2\epsilon)^{\gamma^2/2} - e^{\gamma h_\epsilon(x)} (\epsilon)^{\gamma^2/2})(e^{\gamma h_{2\epsilon}(y)} (2\epsilon)^{\gamma^2/2} - e^{\gamma h_\epsilon(y)} (\epsilon)^{\gamma^2/2})\right] dx dy \\ &= \int_{A \times A} \mathbb{E}\left[(e^{\gamma(h_\epsilon(x)+h_\epsilon(y))} \epsilon^{\gamma^2})(2^{\gamma^2/2} e^{\gamma(h_{2\epsilon}(x)-h_\epsilon(x))} - 1)(2^{\gamma^2/2} e^{\gamma(h_{2\epsilon}(y)-h_\epsilon(y))} - 1)\right] dx dy \end{aligned}$$

When $|x - y| > 4\epsilon$, we know that tree terms in the expectation are independent since they use the information respectively in $B_\epsilon(x) \cup B_\epsilon(y)$, $B_{2\epsilon}(x) \setminus B_\epsilon(x)$, $B_{2\epsilon}(y) \setminus B_\epsilon(y)$ and the three parts are disjoint. Therefore we can do factorize the expectation. Moreover the fact that the density is martingale implies that

$$\begin{aligned} &\mathbb{E}\left[(e^{\gamma(h_\epsilon(x)+h_\epsilon(y))} \epsilon^{\gamma^2})(2^{\gamma^2/2} e^{\gamma(h_{2\epsilon}(x)-h_\epsilon(x))} - 1)(2^{\gamma^2/2} e^{\gamma(h_{2\epsilon}(y)-h_\epsilon(y))} - 1)\right] \\ &= \mathbb{E}\left[e^{\gamma(h_\epsilon(x)+h_\epsilon(y))} \epsilon^{\gamma^2}\right] \mathbb{E}\left[2^{\gamma^2/2} e^{\gamma(h_{2\epsilon}(x)-h_\epsilon(x))} - 1\right] \mathbb{E}\left[2^{\gamma^2/2} e^{\gamma(h_{2\epsilon}(y)-h_\epsilon(y))} - 1\right] \\ &= 0, \forall |x - y| > 4\epsilon \end{aligned}$$

Therefore, it suffices to consider the part that $|x - y| \leq 4\epsilon$,

$$\begin{aligned} &\mathbb{E}\left[|\mu_{2\epsilon}^\gamma(A) - \mu_\epsilon^\gamma(A)|^2\right] \\ &\leq \int_{|x-y| \leq 4\epsilon} \mathbb{E}\left[(e^{\gamma h_{2\epsilon}(x)} (2\epsilon)^{\gamma^2/2} - e^{\gamma h_\epsilon(x)} (\epsilon)^{\gamma^2/2})(e^{\gamma h_{2\epsilon}(y)} (2\epsilon)^{\gamma^2/2} - e^{\gamma h_\epsilon(y)} (\epsilon)^{\gamma^2/2})\right] dx dy \\ &\leq C\epsilon^2 \left[\mathbb{E}[e^{2\gamma h_{2\epsilon}(x)} (2\epsilon)^{\gamma^2}] + \mathbb{E}[e^{2\gamma h_\epsilon(x)} (\epsilon)^{\gamma^2}]\right] \\ &= 2C\epsilon^{2-\gamma^2} \end{aligned}$$

When $\gamma < \sqrt{2}$, this error converges to 0 so the sequence is a Cauchy sequence in L^2 . Using the Borel-Cantalli lemma, this implies that for any compact A , the sub-sequence converges almost surely to a limit $\mu^\gamma(A)$. The L^2 estimation gives also the uniform speed of convergence so μ^γ gives a limit measure. \square

3.7 γ -thick point

Theorem 3.7.1 (γ -thick point). *On the domain D , if we sample a point after the Liouville measure $\mu^\gamma(dz)$, then almost surely*

$$\lim_{\epsilon \rightarrow 0} \frac{h_\epsilon(z)}{\log 1/\epsilon} = \gamma.$$

Recall the property of Brownian motion

$$\frac{B_t}{t} \xrightarrow{a.s.} 0$$

and the fact that $h_{e^{-t}}(z)$ is a Brownian motion, for a point z fixed, we have

$$\lim_{\epsilon \rightarrow 0} \frac{h_\epsilon(z)}{\log 1/\epsilon} = 0.$$

It seems a little paradox, however this is a sample for fix point. If we do sample by the Liouville measure, since the measure it self is random, the point with larger mass has more chance to be chosen, so it changes the typical point. In the proof, we will see how to find this change of probability.

Proof. The Liouville measure gives, in fact, double sample where a hidden sample is for GFF. The joint distribution is

$$Q(d\mu, dh) = \frac{1}{Z_\gamma} e^{\gamma h} dz dh$$

where $e^{\gamma h}$ represents the Liouville measure defined in the last section and dh means density of GFF and

$$Z_\gamma = \mathbb{E} \left[\int_D e^{\gamma h(z)} dz \right].$$

Then, the measure conditional of GFF when a point is fixed (called rooted measure in some reference) is

$$Q(dh|d\mu) = \frac{Q(dh, d\mu)}{Q(d\mu)} = \frac{\frac{1}{Z_\gamma} e^{\gamma h} dz dh}{\mathbb{E}_h \left[\frac{1}{Z_\gamma} e^{\gamma h} dz dh \right]}$$

3. GAUSSIAN FREE FIELD AND LIOUVILLE QUANTUM GRAVITY 30

$$\begin{aligned}
 \mathbb{E}_h\left[\frac{1}{Z_\gamma}e^{\gamma h}dzdh\right] &= \lim_{\epsilon \rightarrow 0} \frac{1}{Z_\gamma} \mathbb{E}[e^{\gamma h_\epsilon(z)}\epsilon^{\gamma^2/2}]dz \\
 &= \frac{1}{Z_\gamma}(R(z, D))^{\gamma^2/2}dz \\
 \Rightarrow Q(dh|dz) &= e^{\gamma h}(R(z, D))^{-\gamma^2/2}dh \\
 &= \lim_{\epsilon \rightarrow 0} e^{\gamma h_\epsilon}\epsilon^{\gamma^2/2}(R(z, D))^{-\gamma^2/2}dh
 \end{aligned}$$

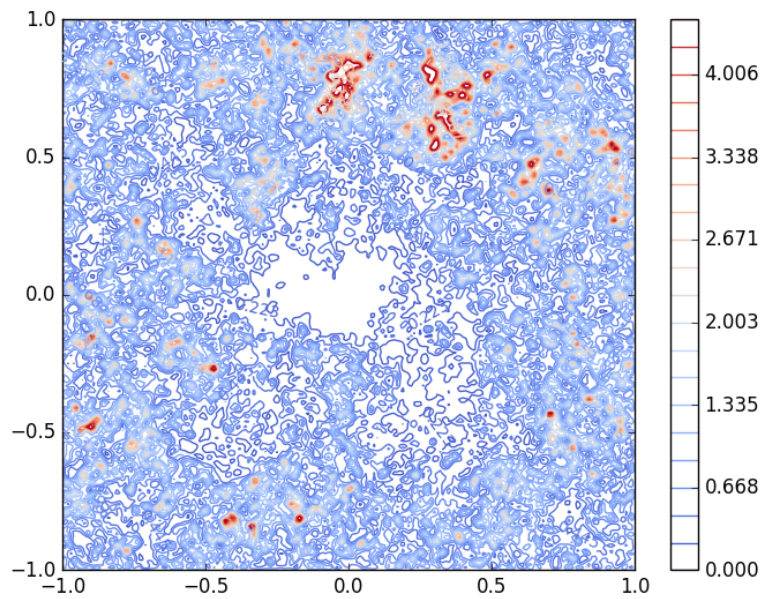
Applying the theorem of Gisarnov, this implies that under the Liouville measure and restricted on the circle average, the GFF \tilde{h}_ϵ has a change of probability $\tilde{h}_\epsilon = h_\epsilon + \gamma \log \epsilon$. Therefore

$$\lim_{\epsilon \rightarrow 0} \frac{\tilde{h}_\epsilon(z)}{\log 1/\epsilon} = \gamma.$$

□

4

Gaussian multiplicative chaos theory



In the construction of LQG, the usage of circle average aims at approximation of the random distribution and to make sense the $e^{\gamma h}$. However, as we have seen the canonical construction of GFF as

$$h = \sum_{i=1}^{\infty} X_i e_i$$

, one may ask a natural question : Can we do approximation naturally

by just truncation of terms ? Thus we define $h_n = \sum_{i=1}^n X_i e_i$ and then define a density and finally pass n to infinity.

This intuition is natural since these two approximations are always used in the domain of analysis and PDE, with the terminology called **modification by convolution** for type like circle average and **truncation of frequency** for type of approximation above. The two techniques could be used to treat Schwartz distribution like functions and get some fine estimation of operator and embedding of function space of L^P and Soblev etc.

We return to the original question. The answer is positive and in fact, J.P Kahane has developed a complete theory called **Gaussian multiplicative chaos** ("Le chaos multiplicatif" in french) in 80th [Kah85], [Kah87] to study the model of the cascade of Mandelbrot. Informally speaking, given a family of Gaussian process $\{Y_n(x)\}_{n \geq 0}$ where $\{Y_n\}_{n \geq 0}$ are independent but $Y_n(x)$ indexed by the position $x \in D$ associate covariance K_n such that

$$\mathbb{E}[Y_n(x)Y_n(y)] = K_n(x, y)$$

If we denote $X_n(x) = \sum_{k=0}^n Y_k(x)$, we know that $e^{\gamma X_n(x) - \frac{\gamma^2}{2} \mathbb{E}[X_n^2(x)]}$ defines a martingale. We treat it as the density at the position x . This is why it is called Gaussian multiplicative chaos : the density is random and is designed level by level

$$e^{\gamma X_n(x) - \frac{\gamma^2}{2} \mathbb{E}[X_n^2(x)]} = \prod_{i=0}^n e^{\gamma Y_i(x) - \frac{\gamma^2}{2} \mathbb{E}[Y_i^2(x)]}$$

. If $\forall x, y \in D, \sum_{n=0}^{\infty} K_n < \infty$, the X_n converge in L^2 to a Gaussian process and we could define the limit density directly. However, when $\sum_{n=0}^{\infty} K_n$ doesn't converge simply, the limit of this density could be well defined ?

This is the motivation of the theory of Gaussian multiplicative chaos theory and it's the same question when we define the LQG. The following part includes some basic definitions and propositions about this theory. It has a very nice frame and may be more general than GFF and LQG theory in some sense. Some parts look parallel as what has been developed in the precedent chapter, but with a different viewpoint. The content is based on the video by Rémi Rhodes during the workshop of random geometry at Issac Newton Institute and [RV⁺14] and the original article [Kah85].

4.1 Basic frame

In this section, we give the general frame of the Gaussian multiplicative chaos. We will introduce an important comparison inequality, then σ -

positive kernel which allows us to prove the uniqueness.

4.1.1 Comparison inequality

The first part is conserved for the comparison inequality and it is always listed at first in the review of Rémi Rhodes since it is much used in the proof.

Lemma 4.1.1 (Comparison inequality). *Given $\{A_i\}_{1 \leq i \leq n}, \{B_i\}_{1 \leq i \leq n}$ two centered Gaussian vectors which satisfy*

$$\forall 1 \leq i, j \leq n, \mathbb{E}[A_i A_j] \leq \mathbb{E}[B_i B_j]$$

then $\forall F : \mathbb{R}_+ \rightarrow \mathbb{R}$ convex and $p_i \geq 0$

$$\mathbb{E}\left[F\left(\sum_{i=1}^n p_i e^{A_i - \frac{1}{2}\mathbb{E}[A_i^2]}\right)\right] \leq \mathbb{E}\left[F\left(\sum_{i=1}^n p_i e^{B_i - \frac{1}{2}\mathbb{E}[B_i^2]}\right)\right]$$

.

Remark. In this section, we will use it to prove the uniqueness of limit measure in context of σ -positive kernel. However, this inequality is much more powerful since it still works in other situation out of the frame of σ -positive kernel

4.1.2 σ -positive kernel

A nice frame to study the limit measure is the condition σ -positive kernel.

Definition 4.1.1 (σ -positive kernel). Take a locally compact metric space (D, d) and a function $K : D \times D \rightarrow \mathbb{R}_+$ is said to be σ -positive type if

$$K(x, y) = \sum_{n \geq 0} K_n(x, y)$$

where K_n is nice : it is continuous, positive, and positive definite. So it is associated with a sequence of independent Gaussian process $\{Y_n(\cdot)\}_{n \geq 0}$ such that $K_n(x, y) = \mathbb{E}[Y_n(x)Y_n(y)]$

We define the approximated measure by the the partial sum.

Definition 4.1.2 (Approximated measure). Given a Radon measure μ associated to the metric space (D, d) , we define $X_n(x) = \sum_{i=0}^n X_i(x)$ and the approximated measure $M_n(dx) = e^{X_n(x) - \frac{1}{2}\mathbb{E}[X_n^2(x)]} \mu(dx)$.

More generally, we define $M_n^\gamma(dx) = e^{\gamma X_n(x) - \frac{\gamma^2}{2}\mathbb{E}[X_n^2(x)]} \mu(dx)$.

We give some simple observation. $\forall A \subset D$ compact subset, $\{M_n(A)\}_{n \geq 0}$ is a martingale positive with respect to the filtration

$$\mathcal{F}_n = \sigma(\{Y_i(x), x \in D, 0 \leq i \leq n\})$$

thanks to the independent increment. Therefore, $M_n(A) \xrightarrow{n \rightarrow \infty} M(A)$ a.s, which implies

$$M_n(dx) \xrightarrow{n \rightarrow \infty} M(dx) \text{ a.s}$$

convergence to a Radon measure in weak sense of Schwartz distribution i.e

$$\text{a.s } \omega, \forall f \in C_b(A), M_n(f) \xrightarrow{n \rightarrow \infty} M(f)$$

However, the limit measure may be trivial : we only have

$$\mathbb{E}[M(A)] \leq \mathbb{E}[M_n(A)] = \mu(A)$$

, but not necessarily the convergence L^1 or we don't know if this martingale is U.I. We remark that thanks to the lemma of Schéffa, it suffices to prove that $\mathbb{E}[M(A)] = \mu(A)$.

Another question is whether the limit depends on how we decompose the K as the sum. So we draw a little summary of question.

Question 1. Is $M(dx)$ trivial ?

Question 2. Is $M(dx)$ unique or it depends on the decomposition of kernel ?

4.1.3 Uniqueness

A first result is that in the context of σ -positive kernel, the limit is unique. Its proof shows how to apply the comparison lemma.

Theorem 4.1.1 (Uniqueness). *The law of M doesn't depend on the σ -decomposition of K .*

Proof. We take two different decomposition $K = \sum_{i \geq 0} K_i = \sum_{i \geq 0} K'_i$ and the Gaussian process associated $\{Y_i\}_{i \geq 0}, \{Y'_i\}_{i \geq 0}$. Because that the sum $\sum_{i=0}^p K_i$ is always increasing, taking A compact and $\epsilon > 0$ and for p' large enough

$$\forall x, y \in A, \sum_{i=0}^p K_i(x, y) \leq \epsilon + \sum_{i=0}^{p'} K'_i(x, y)$$

To utilize the comparison lemma, we denote $X_p = \sum_{i=0}^p Y_i$, $X_{p'} = \sum_{i=0}^{p'} Y'_i$ and one random variable $Z \sim \mathcal{N}(0, 1)$ independent with all the other random variables. Then for any convex function F

$$\mathbb{E}[F(\int_A e^{X_p - \frac{1}{2}\mathbb{E}[X_p^2]} \mu(dx))] = \mathbb{E}[F(\int_A e^{\sqrt{\epsilon}Z - \frac{\epsilon}{2} + X_{p'} - \frac{1}{2}\mathbb{E}[X_{p'}^2]} \mu(dx))]$$

Suppose the martingale is U.I and we pass to the limit of p, p' then we pass $\epsilon \rightarrow 0$ using dominated convergence theorem and obtain

$$\mathbb{E}[F(M(A))] \leq \mathbb{E}[F(M'(A))]$$

We apply the same argument and obtain $\mathbb{E}[F(M(A))] = \mathbb{E}[F(M'(A))]$ and finally we plug in $F = e^{-\lambda x}$ and prove that $M(A)$ and $M'(A)$ has the same law. \square

4.2 Non-degenerate limit measure

In this part, we states the situation when the approximated measure converges U.I to the limit. We will first state the theorem in a most general case and later in \mathbb{R}^d . We still add some necessary remark and some historical background and motivation.

One important theorem will not be discussed, but the base of the following theorem is from [KP76] when studying discrete random cascade. It classifies the limit measure in two case : **non-degenerate** when the martingale $M_n(A)$ is U.I and **degenerate** when the martingale isn't U.I and is 0 almost surely. That is to say

$$\mathbb{E}[M(A)] > 0 \Leftrightarrow \mathbb{E}[M(A)] = \mu(A)$$

. That's the reason why we call degenerate and non-degenerate.

4.2.1 General situation

This part introduce a very general situation in [Kah85]. We will focus on a log-type kernel with a good calls of measure.

Definition 4.2.1 (Log-type kernel). A kernel K is defined as log-type if and only if $\forall x, y \in D$

$$K(x, y) = \log_+ \frac{1}{d(x, y)} + g(x, y)$$

where g is bounded in $D \times D$ and $\log_+(\cdot) = \log(\cdot) \vee 0$.

Remark. Log-type kernel is also the case met when defining 2D GFF, since the Green function as the kernel is log-type.

Definition 4.2.2 (Class R_α^+ ($\alpha > 0$)). A Borel measure μ is of class R_α^+ if and only if $\forall \epsilon > 0, \exists$ compact set A_ϵ depending on $\epsilon, \exists \delta > 0, C > 0$ such that

- $\mu(D \setminus A_\epsilon) \leq \epsilon$
- $\forall O$ open, $\mu(O \cap A_\epsilon) \leq C \text{diam}(O)^{\alpha+\delta}$.

Definition 4.2.3 (β -energy). A Borel measure μ defined on D is said of β -energy if

$$I_\beta(\mu) = \int \int_{D \times D} \frac{1}{d(x, y)^\beta} \mu(dx) \mu(dy) < \infty$$

Remark. $I_\beta(\mu) < \infty \Rightarrow \mu \in R_\alpha^+, \forall 0 < \alpha < \beta$.

This definition seems very technical since J.P Kahane extend his theory on perfect set in [Kah85]. Using this definition, he obtains a nice and very general theorem.

Theorem 4.2.1. Assume K a σ -positive kernel of log-type and a measure $\mu \in R_\alpha^+$. If $\gamma^2 < 2\alpha$, then the martingale $M_{n,\gamma}(A)$ is U.I. and its limit measure $M_\gamma \in R_{\alpha - \frac{\gamma^2}{2}}^+$

Remark. This theorem also implies that M_γ has no atoms.

Remark. J.P Kahane has also studied a necessary condition, which is subtle and interacts with the doubling volume condition in harmonic analysis.

4.2.2 Case in \mathbb{R}^d

In this subsection, we apply the general theorem in \mathbb{R}^d . Before starting, as what we have done in LQG, we can also obtain the L^2 theorem easily if K is of log-type since

$$\begin{aligned} \mathbb{E}[M_{n,\gamma}(A)^2] &= \mathbb{E}\left[\int_{A \times A} e^{\gamma X_n(x) + \gamma X_n(y) - \frac{\gamma^2}{2} \mathbb{E}[X_n^2(x)] - \frac{\gamma^2}{2} \mathbb{E}[X_n^2(y)]} \mu(dx) \mu(dy)\right] \\ &= \int_{A \times A} e^{\gamma^2 \sum_{i=0}^n K_i(x,y)} \mu(dx) \mu(dy) \\ &\leq \int_{A \times A} e^{\gamma^2 \sum_{i=0}^\infty K_i(x,y)} \mu(dx) \mu(dy) \\ &\leq C \int_{A \times A} e^{\gamma^2 \log_+ \frac{1}{d(x,y)}} \mu(dx) \mu(dy) \\ &= C \int_{A \times A} \frac{1}{d(x,y)^{\gamma^2}} \mu(dx) \mu(dy) = C I_{\gamma^2}(\mu) \end{aligned}$$

. In \mathbb{R}^d with Lebesgue measure, we know it's finite if $\gamma^2 < d$, this coincides the L^2 theory in LQG.

However, if we apply the most general theory, we can extend to the situation $\gamma^2 < 2d$ and it's also the range of LQG theory. In conclusion, we states the theorem

Theorem 4.2.2 (Criteria of non-degeneration). *Assume K a σ -positive kernel of log-type and a measure μ is Lebesgue or absolutely continuous with respect to Lebesgue measure. If $\gamma^2 < 2d$, then the martingale $M_{n,\gamma}(A)$ is U.I. and its limit measure M_γ is non-degenerate. If $\gamma^2 \geq 2d$, then it's almost surely 0.*

4.3 Further properties

For further property like the moment estimation, the interested reader can consult the reference [RV⁺14] as review.

4.4 Numerical experience : GFF and Liouville measure on $[0, 1]^2$

In this section, we introduce several interesting numerical methods to simulate GFF. We will use these simulation not only to give an intuitive impression how a GFF looks like, but also to verify the properties like circle average theorem.

4.4.1 GFF on $[0, 1]^2$

We first construct the GFF on $[0, 1]^2$. Noting that a basis of $H_0^1([0, 1]^2)$ is $\{e_{j,k}\}_{j,k \geq 1}$

$$e_{j,k} = \frac{2}{\pi} \frac{1}{\sqrt{j^2 + k^2}} \sin(j\pi x) \sin(k\pi y)$$

.Therefore, a GFF can be generated by

$$h = \sum_{j,k \geq 1} \frac{2}{\pi} \frac{X_{j,k}}{\sqrt{j^2 + k^2}} \sin(j\pi x) \sin(k\pi y)$$

, where $X_{j,k}$ is a family of independent Gaussian. Of course, we cannot do infinite sum and we just do a sum of finite terms. The following image is an instance of GFF to show its figure.

4.4.2 Liouville measure on $[0, 1]^2$

The Liouville measure, however, in our context is just an illustration to show how it looks like. We don't want to do the limit of a sub-series of the circle average of the field, but just do an exponential with also normalization to show how the parameter γ change the form.

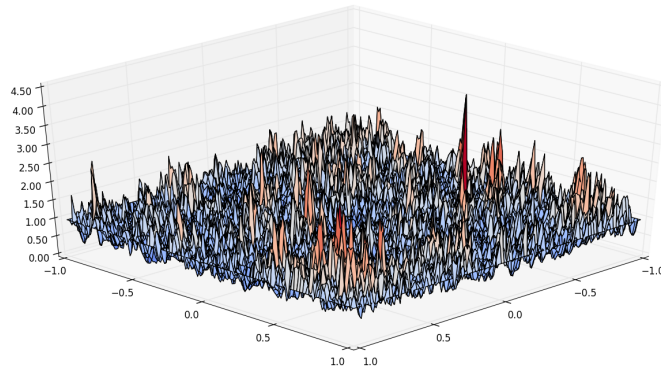


Figure 4.1: A sample of Liouville measure with parameter $\gamma = 0.5$

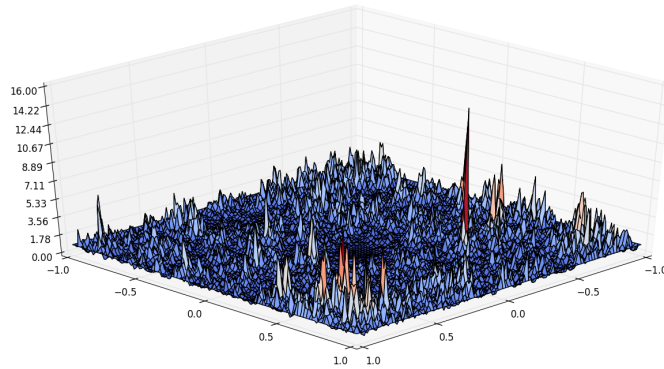
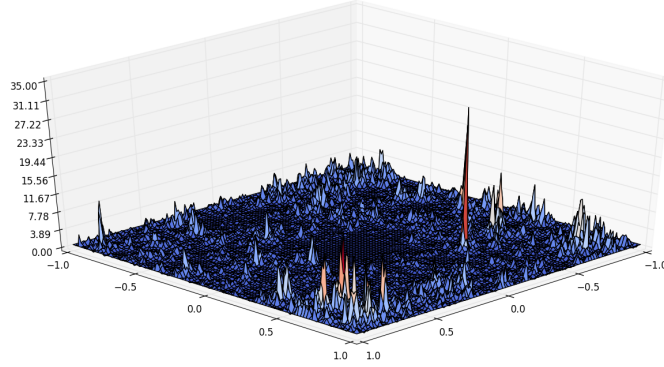
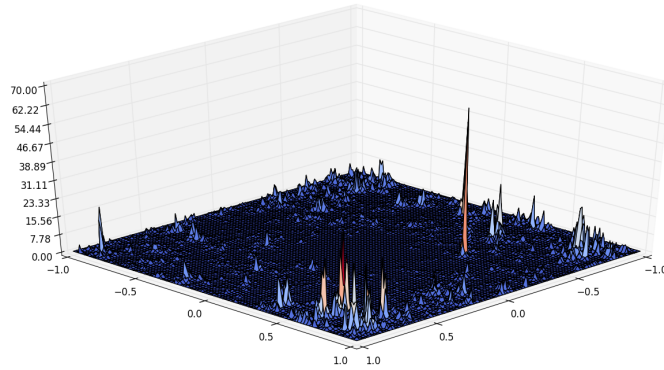


Figure 4.2: A sample of Liouville measure with parameter $\gamma = 1$

From the simulation, we see that the density of Liouville measure looks like the mountains and the bigger γ is, the higher the peak is. Since it is always a density of probability, this means the probability trends to be singular. In fact, when $\gamma > 2$, the Liouville measure becomes trivial since the limit takes only the absolutely continuous

Figure 4.3: A sample of Liouville measure with parameter $\gamma = \sqrt{2}$ Figure 4.4: A sample of Liouville measure with parameter $\gamma \rightarrow 2$

part. This can be seen intuitively from the simulation.

4.4.3 Circle average

Finally, we come to the simulation to verify the circle average theorem. We just take the discrete time on $[0, 1]$ and do the discrete integration centered at 0 of radius e^{-t} . Since the basis has an explicit expression, we can plugin directly position to get the exact value. As the function \sin is very regular, this simulation need a large term of basis in order to see the fractal property of the Brownian motion.

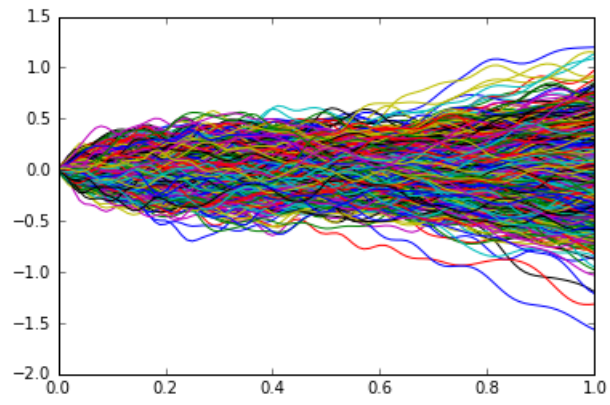
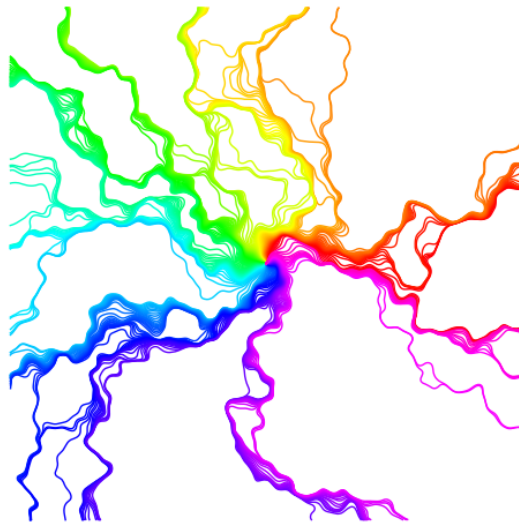


Figure 4.5: A simulation of 1000 traces of $h_{e^{-t}}(0)$ for $t \in \{0, 0.1, 0.2 \cdots 1.0\}$

5

Imaginary geometry



As Brownian motion, who is the brick to build numerous one dimension interesting process and is applied in many domains, the GFF can also be generate many fascinating two dimensional phenomenons. In this chapter, we talk about one called imaginary geometry.

We give a brief introduction of imaginary geometry at first. As the Liouville quantum gravity defines a random measure $e^{\gamma h} dz$, the imaginary geometry would like make sense a random vector field $e^{ih/\chi}$. We meet the same problem how to explain a field defined by a distribution. This time, the construction will relate the SLE process. The interest of this subject is that $e^{ih/\chi}$ will induce some random flow with

the non-standard behaviors, for example, some times two flows will cut and then be merged under certain situation.

This chapter is organized as following : we explain some story about the flow defined in domain to give some intuition why SLE should be a candidate of the flow line. Then we introduce at first the key technique of coupling of SLE/GFF and its variants, followed by many interesting properties of $e^{ih/\chi}$ including the flow line, counterflow line, its duality. The last part of this chapter is conserved for numerical simulation. The author would like highlight this part, since it can be seen as an independent section taking the view point of engineer to study the imaginary geometry and almost all the theorem will be illustrated in it. Readers can even jump the part of maths and appreciate the beautiful directly in this section.

The content of this chapter is after a series of article [\[MS16a\]](#),[\[MS+16d\]](#),[\[MS16b\]](#) [\[MS13\]](#). The author is lucky to meet Prof. Miller at Lyon and to learn some trick about how to realize these beautiful images.

5.1 Coupling of GFF and SLE

This section introduce the construction of the flow and the key technique of the coupling between GFF and SLE.

5.1.1 Why the flow should be a SLE ?

As mentioned at first, we would like to study the flow line defined by GFF. Here we give some intuitive explanation why SLE should be the candidate. We first suppose for the instant that h is a continuous real valued function and we define a vector field $e^{ih/\chi}$ on the domain D , where χ is a positive constant and we will explain its meaning later. For the instant, we also suppose that the filed satisfies Liptchitz condition, then the flow η generated by this filed is

$$\frac{d}{dt}\eta(t) = e^{ih(\eta(t))/\chi}.$$

Now, we treat this function h as GFF with maybe some boundary condition, then the conformal invariance and Markov domain property plays an important role, informally speaking, the curve $\eta[t, \infty)$ should also be independent with $\eta[0, t)$ and invariant under the conformal mapping, given that h determines the flow. More precisely, the former comes from the Markov domain property that $h|_{\eta[0, t)}$ and $h|_{\eta[0, t)}^c$ are independent, so $\eta[t, \infty)$ determined by $h|_{\eta[0, t)}^c$ should be independent

with the former. The latter inherits directly from the conformal invariance of GFF. If we denote a conformal mapping $f_t : \mathbb{H} \setminus \eta[0, t) \rightarrow \mathbb{H}$, $f_t(\eta[t, \infty))$ should also be a flow determined by GFF, so it should be the type of SLE curve.

The next question is that which SLE can be coupled with the GFF. Suppose $\phi : (\tilde{D}, \tilde{h}) \rightarrow (D, h)$ which means a conformal mapping $\phi : \tilde{D} \rightarrow D$ and the fields generate the same flow after conformal mapping

$$\begin{aligned} \eta &= \phi \circ \tilde{\eta} \\ \frac{d}{dt}\eta(t) &= e^{ih(\eta(t))/\chi} \\ \frac{d}{ds}\tilde{\eta}(s) &= e^{ih(\tilde{\eta}(s))/\chi} \end{aligned}$$

Here t, s means different parametrizations. These equations induce the relation

$$e^{ih(\eta(t))/\chi} = \frac{d}{dt}(\phi \circ \tilde{\eta}(s)) = \phi'(\tilde{\eta}(s)) \frac{d}{ds}(\tilde{\eta}(s)) \frac{ds}{dt} = \phi'(\tilde{\eta}(s)) e^{ih(\tilde{\eta}(s))/\chi} \frac{ds}{dt}$$

Then we get the identity

$$h \circ \phi - \chi \arg(\phi') = \tilde{h} \tag{5.1}$$

and the property of Markov domain and conformal invariance translates as

$$h \circ f_t - \chi \arg(f_t') \stackrel{d}{=} h \tag{5.2}$$

This identity inspires us to look for a proper SLE and the parameters remain to be fixed.

5.1.2 Theorem of coupling

Main task of this part is to treat the theorem of GFF/SLE coupling.

We recall the definition of chordal SLE_κ for $0 < \kappa \leq 4$ is a simple curve η whose associated conformal mapping $g_t : \mathbb{H} \setminus \eta[0, t] \rightarrow \mathbb{H}$ satisfies

$$\partial_t g_t(z) = \frac{2}{g_t(z) - U_t}$$

where $U_t = \sqrt{\kappa} B_t$ and B_t is a standard Brownian motion. We define $f_t = g_t - U_t$. Then it satisfies

$$\partial_t f_t(z) = \frac{2}{f_t(z)} - U_t.$$

Theorem 5.1.1 (GFF/SLE coupling). *Given $\kappa \in (0, 4]$ and f_t defined as the flow of mapping of SLE_κ above. A constant χ is designed $\chi = \frac{2}{\sqrt{\kappa}} - \frac{\sqrt{\kappa}}{2}$ and we define a harmonic function Θ_t to add the boundary condition*

$$\begin{aligned}\Theta_0(z) &= \frac{\pi}{\sqrt{\kappa}} - \frac{2}{\sqrt{\kappa}} \arg(z) \\ \Theta_t(z) &= \Theta_0(f_t(z)) - \chi \arg(f'_t(z)) \\ &= \frac{\pi}{\sqrt{\kappa}} - \frac{2}{\sqrt{\kappa}} \arg(f_t(z)) - \chi \arg(f'_t(z)).\end{aligned}$$

Then we construct the GFF $h = \tilde{h} + \Theta_0$ where \tilde{h} is a GFF on \mathbb{H} with null boundary condition. This GFF satisfies the identity

$$h \circ f_t - \chi \arg(f'_t) \stackrel{d}{=} h$$

Using this theorem, a SLE and a GFF can be coupled, namely they are mutually determined.

Proof. It suffices to prove that $\forall \phi \in C_0^\infty(\mathbb{H})$

$$\langle h, \phi \rangle \stackrel{d}{=} \langle h \circ f_t - \chi \arg(f'_t), \phi \rangle$$

and we know the LHS is just a Gaussian. So we apply the characteristic function to the RHS. We remark that the expectation has two part : the expectation with respect to the GFF \tilde{h} and that with respect to the Brownian motion who generates the SLE.

$$\mathbb{E}_{h,B}[\exp(i\theta \langle h \circ f_t - \chi \arg(f'_t) + \tilde{h} \circ f_t, \phi \rangle)] = \mathbb{E}_B[\exp(im_t \theta - \frac{1}{2} \sigma_t^2 \theta^2)]$$

where

$$\begin{aligned}m_t &= \left\langle \frac{\pi}{\sqrt{\kappa}} - \frac{2}{\sqrt{\kappa}} (\text{Im} \log(f_t)) - \chi \text{Im} \log(f'_t), \phi \right\rangle \\ \sigma_t^2 &= \text{Var}(\langle \tilde{h} \circ f_t, \phi \rangle).\end{aligned}$$

We will prove $\exp(im_t \theta - \frac{1}{2} \sigma_t^2 \theta^2)$ is a martingale, so the expectation coincide at time 0 and at time t . This can be done by two steps : 1, m_t is a local martingale. 2, $d\langle m_t \rangle = -d(\sigma_t^2)$.

Step 1 - m_t is a local martingale: We know that

$$m_t = \left\langle \frac{\pi}{\sqrt{\kappa}} - \frac{2}{\sqrt{\kappa}} (\text{Im} \log(f_t)) - \chi \text{Im} \log(f'_t), \phi \right\rangle.$$

Using the formula of Ito

$$\begin{aligned} d(\log f_t(z)) &= \left(\frac{4 - \kappa}{2f_t^2(z)} \right) dt - \left(\frac{\sqrt{\kappa}}{f_t(z)} \right) dB_t \\ d(f_t'(z)) &= \frac{d}{dz}(\partial_t f_t(z)) = \frac{-2f_t'(z)}{f_t^2(z)} dt \\ d(\log f_t'(z)) &= \frac{1}{f_t'(z)} d(f_t'(z)) = \frac{-2}{f_t^2(z)} dt \end{aligned}$$

and we combine them together

$$\begin{aligned} & d \left[\frac{\pi}{\sqrt{\kappa}} - \frac{2}{\sqrt{\kappa}} (\operatorname{Im} \log(f_t(z))) - \chi \operatorname{Im} \log(f_t'(z)) \right] \\ &= -\frac{2}{\sqrt{\kappa}} \operatorname{Im} \left(\frac{4 - \kappa}{2f_t^2(z)} dt - \frac{\sqrt{\kappa}}{f_t(z)} dB_t \right) - \chi \operatorname{Im} \left(\frac{-2}{f_t^2(z)} \right) dt \\ &= -\operatorname{Im} \left(\frac{2}{f_t(z)} \right) dB_t \end{aligned}$$

Therefore, $dm_t = \langle -\operatorname{Im} \left(\frac{2}{f_t(z)} \right), \phi \rangle dB_t$ is a local martingale.

Step 2 - $d\langle m_t \rangle = -d\langle \sigma_t^2 \rangle$: We apply the result of step 1

$$d\langle m_t \rangle = \int_{\mathbb{H} \times \mathbb{H}} \phi(x)\phi(y) \operatorname{Im} \left(\frac{2}{f_t(x)} \right) \operatorname{Im} \left(\frac{2}{f_t(y)} \right) dx dy.$$

Using the change of variable for the distribution and Green function

$$\begin{aligned} \sigma_t^2 &= \operatorname{Var}(\langle \tilde{h} \circ f_t, \phi \rangle) \\ &= \operatorname{Var}(\langle \tilde{h}, \phi \circ f_t^{-1} \det(f_t')^{-1} \rangle) \\ &= \int_{\mathbb{H} \times \mathbb{H}} \phi \circ f_t^{-1}(u) \phi \circ f_t^{-1}(v) G_{\mathbb{H}}(u, v) \det(f_t')^{-2} du dv \\ &= \int_{\mathbb{H} \times \mathbb{H}} \phi(x)\phi(y) G_{\mathbb{H}}(f_t(x), f_t(y)) dx dy. \end{aligned}$$

Therefore, we obtain that

$$-d\langle \sigma_t^2 \rangle = -d \left[\int_{\mathbb{H} \times \mathbb{H}} \phi(x)\phi(y) \partial_t G_{\mathbb{H}}(f_t(x), f_t(y)) dx dy \right].$$

What we need to do is just to calculate the derivative with respect to time of Green function. The formula of Green function for \mathbb{H} is explicit $G_{\mathbb{H}}(a, b) = -\log \left| \frac{a-b}{x-b} \right|$, so

$$\begin{aligned} \partial_t G_{\mathbb{H}}(f_t(x), f_t(y)) &= -\operatorname{Re} \partial_t \left[\log(f_t(x) - f_t(y)) - \log(f_t(x) - \overline{f_t(y)}) \right] \\ &= -\operatorname{Im} \left(\frac{2}{f_t(x)} \right) \operatorname{Im} \left(\frac{2}{f_t(y)} \right). \end{aligned}$$

Hence we obtain the result that we wanted.

Finally, we justify how two random object can be coupled. We develop the formula

$$h \stackrel{d}{=} \frac{\pi}{\sqrt{\kappa}} - \frac{2}{\sqrt{\kappa}} \arg(f_t(z)) - \chi \arg(f'_t) + \tilde{h} \circ f_t. \quad (5.3)$$

So, we sample at first a Brownian motion B_t and use it to generate a SLE_κ curve $\eta[0, \infty)$. Then we sample a GFF \tilde{h} on $\mathbb{H} \setminus \eta[0, \infty)$. We apply the formula in the RHS and then we get a GFF on the upper-half plane. Informally, we utilize the information of a Brownian motion plus the information of the complement, then they compose a entire GFF. However, determining a SLE by a GFF requires the coupling of reversed flow discussed in the following subsection. \square

Remark. Reader may wonder why we don't construct the flow line by the circle average $e^{ih_\epsilon/\chi}$. This is a natural idea but the this question is still open except for the level line case proved in [SS09], [SS13].

Except the discussion in the preceding subsections, this construction gives us more information why the SLE process can be regarded as the flow line. We fix the time T and suppose once again the SLE process is a "regular" curve, observing $f_T(\eta(t))$ moves along the real axis toward right,

$$\begin{aligned} ce^{i0} &= \frac{d}{dt} f_T(\eta(t)) = f'_T(\eta(t)) \frac{d}{dt} \eta(t) \\ &\Rightarrow \arg\left(\frac{d}{dt} \eta(t)\right) = -\arg f'_T(\eta(t)) \end{aligned}$$

So the flow line moves along the direction $-\arg f'_T(\eta(t))$. This value can be calculated by (5.3) and we take the approach from left and from right of the curve, we obtain

$$\begin{aligned} z \rightarrow \eta^-, -\arg(f'_T(\eta(t)-)) &= h/\chi + \frac{\pi}{\sqrt{\kappa}\chi} \\ z \rightarrow \eta^+, -\arg(f'_T(\eta(t)+)) &= h/\chi - \frac{\pi}{\sqrt{\kappa}\chi}. \end{aligned}$$

Informally, the vector field isn't continuous and it has a gap, but the flow line trend to move along its average of left side and right side just like "struggling to find a correct in the turbulence of vector field".

5.2 Flow line, monotony, merging, crossing and light cone

As mentioned in last section, one can identify the coupling between a SLE curve and a GFF as a flow line. In this section, we will describe some interesting phenomenon if we couple several SLE curves in a given GFF.

We denote a SLE type curve η_x^θ if it starts from point x and has an initial "angle" θ , which can be interpreted by adding one constant on GFF h . The interesting phenomenon can be described best by the following three images.

Proposition 5.2.1 (Monotony, merging and crossing). *We couple two SLE type curves $\eta_{x_1}^{\theta_1}$ and $\eta_{x_2}^{\theta_2}$ with a GFF h . Then under some suitable condition, we have three phenomenon are called respectively **monotony**, **merging and crossing** of the flow lines.*

1. *Two flow lines of $\eta_{x_1}^{\theta_1}$ and $\eta_{x_2}^{\theta_2}$ where $x_1 \geq x_2, \theta_1 < \theta_2$. Then $\eta_{x_1}^{\theta_1}$ is always on the right hand side of $\eta_{x_2}^{\theta_2}$. They may meet each other, but once they meet, they will rebound instead of crossing.*
2. *Two flow lines of $\eta_{x_1}^{\theta_1}$ and $\eta_{x_2}^{\theta_2}$ where $x_1 \geq x_2, \theta_1 = \theta_2$. Then once $\eta_{x_1}^{\theta_1}$ and $\eta_{x_2}^{\theta_2}$ meet each other, they will merge and then evolve in a same trace.*
3. *Two flow lines of $\eta_{x_1}^{\theta_1}$ and $\eta_{x_2}^{\theta_2}$ where $x_1 \geq x_2, \theta_1 = \theta_2$. Then once $\eta_{x_1}^{\theta_1}$ and $\eta_{x_2}^{\theta_2}$ meet each other, they will merge and then evolve in a same trace.*

Remark. Here we don't give what the "suitable condition" is, but reader can check [MS16a]. As the phase diagram of SLE is in fact hidden in the Bessel process, the geometrical property of the evolution of more general SLE type curves ($SLE_\kappa(\rho)$) is connected also to some stochastic equation. The related work can be found in [Dub05], [Dub09].

The proof of them depends heavily on one definition called **local set** of GFF. Here we give its definition. To define it, we recall that all the closed subset of domain D

$$\Gamma = \{K \subset \bar{D}, \text{closed}\}$$

form a metric space equipped with the Hausdorff distance

$$d^D(S_1, S_2) = \inf\{\epsilon > 0 | S_1 \subset B(S_1, \epsilon), S_2 \subset B(S_2, \epsilon)\}$$

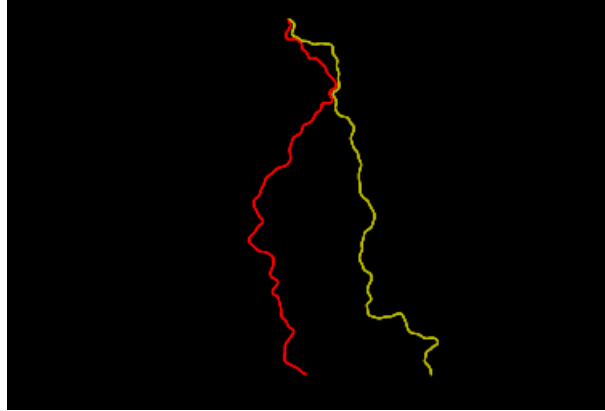


Figure 5.1: Two flow lines of $\eta_{x_1}^{\theta_1}$ (yellow) and $\eta_{x_2}^{\theta_2}$ (red) where $x_1 \geq x_2, \theta_1 < \theta_2$. Then $\eta_{x_1}^{\theta_1}$ is always on the right hand side of $\eta_{x_2}^{\theta_2}$. They may meet each other, but once they meet, they will rebound instead of crossing.

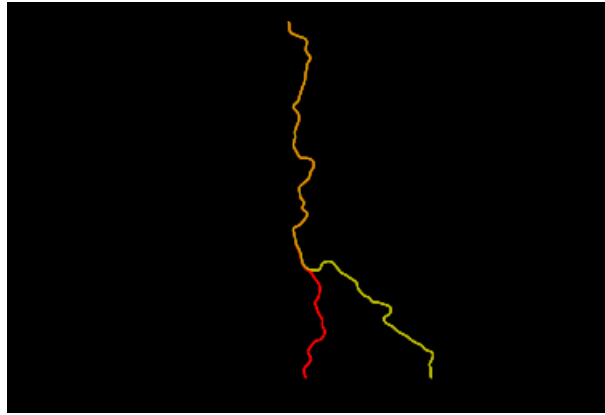


Figure 5.2: Two flow lines of $\eta_{x_1}^{\theta_1}$ (yellow) and $\eta_{x_2}^{\theta_2}$ (red) where $x_1 \geq x_2, \theta_1 = \theta_2$. Then once $\eta_{x_1}^{\theta_1}$ and $\eta_{x_2}^{\theta_2}$ meet each other, they will merge and then evolve in a same trace.

Definition 5.2.1 (Local set). A Γ valued random variable A is said a local set of GFF h if we can sample h by the following steps.

1. Sample (A, h_1) where h_1 is harmonic on $D \setminus A$.
2. Given (A, h_1) , we sample a GFF h_2 on $D \setminus A$.

We set $h = h_1 + h_2$.

Remark. In other word, it is a 2D version strong Markov property and formally, $h - h|A$ has the same law of a GFF on $D \setminus A$ independent of \mathcal{F}_A .

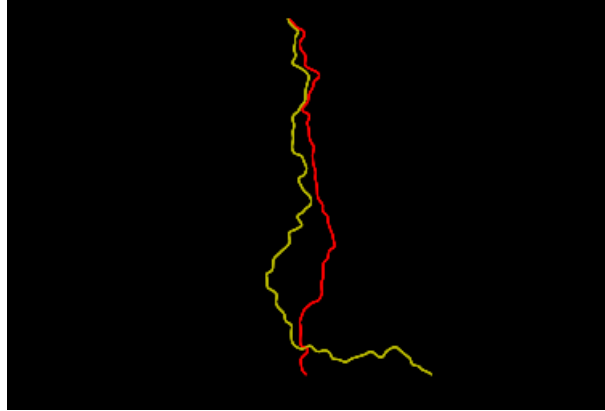


Figure 5.3: Two flow lines of $\eta_{x_1}^{\theta_1}$ (yellow) and $\eta_{x_2}^{\theta_2}$ (red) where $x_1 \geq x_2, \theta_1 > \theta_2$. Then once $\eta_{x_1}^{\theta_1}$ and $\eta_{x_2}^{\theta_2}$ meet each other, one will cross the other. However, the crossing like that happens at most one time.

We know some examples of local sets like a deterministic compact set and in this case, it becomes just the domain Markov property. A non-trivial example of local set is the SLE type curve. This is clear from the SLE/GFF coupling property. The following lemma gives more local set.

Lemma 5.2.1. *Two local sets A_1, A_2 are local sets which are independent conditionally given h , then $A_1 \cup A_2$ is local set of h .*

Finally, we describe some ideas behind these propositions. All the case can be reduced to study the flow line starting from a common point with different angles. Because the SLE type curves are local sets, then when they meet, we condition all the path before meeting, then we only need to study the trace after meeting, and the three situations are the cases.

There are also numerous more sophisticated phenomenon by combining the situations above, for example, starting from every point on the plane by adding two angles $-\frac{\pi}{2}, \frac{\pi}{2}$ and one get so called **mating of trees**, or starting from one point with all the possible angles to get so called **SLE fan**.

5.2.1 Define a flow line by real method ?

Last but not least, we would like ask a question : Could we get the imaginary geometry by real method i.e make sense from differential equation ?

$$\frac{d}{dt}\eta(t) = e^{ih(\eta(t))/\chi}.$$

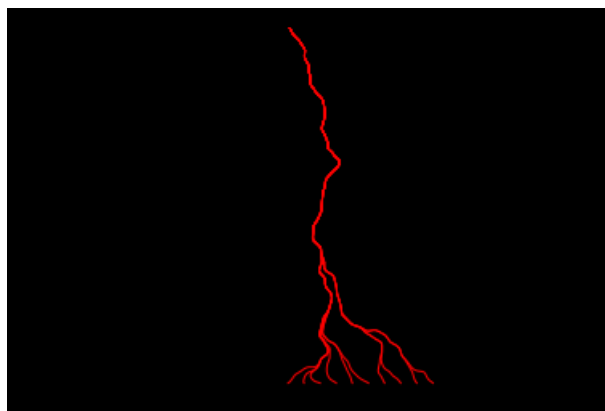


Figure 5.4: A simulation of flow lines starting from different point with a same angle. There will finally be a coalescence. If the angle is $\frac{\pi}{2}$, it's one branch of mating of trees.



Figure 5.5: A simulation of flow lines starting from one point with different angles represented by the colors.

In fact, what we have seen of the numerical simulation in last section is a little cheating : the program never implements a conformal map of Loewner flow, but just iterates the ODE above. Then this the propositions are more or less natural : a real flow just performs like that by Cauchy-Liptchitz theorem. So what has happened ? The flow line looks like a regular flow disturbed by some noise in the medium and becomes zigzag.

If we could make sense this equation, we will not only make sense our simulation, but also another proof all all the proposition above.

Moreover, we may have another construction of SLE without Loewner flow...

5.3 Numerical experience : Flow line of GFF on unit disk

The numerical simulation for imaginary geometry is perhaps mostly significant since it not only gives us a direct impression, but also help us find the properties and do experience. Moreover, from the algorithm of simulation, one get another interpretation of role play by GFF in imaginary geometry.

The object is to simulate the flow and counterflow of a random vector field $e^{ih/\chi}$. We would like to realize it on the domain D . Using the preceding formula 5.3, 5.1 and we suppose that $\phi : D \rightarrow \mathbb{H}$

$$h_D = \tilde{h} \circ \phi - \frac{2}{\sqrt{\kappa}} \arg(\phi) - \chi \arg(\phi') + \frac{\pi}{\sqrt{\kappa}} \quad (5.4)$$

Here, $\tilde{h} \circ \phi$ is just a GFF on domain D with null boundary condition. A direct interpretation is that the vector field without this term is a classical vector field, while this terms gives a random perturbation and changes the direction of the flow. Given a vector field, the simulation of the flow line is direct by ODE system. Thus, we focus on how to choose a good domain so that the conformal mapping ϕ is easy to realize and how to generate a GFF on domain.

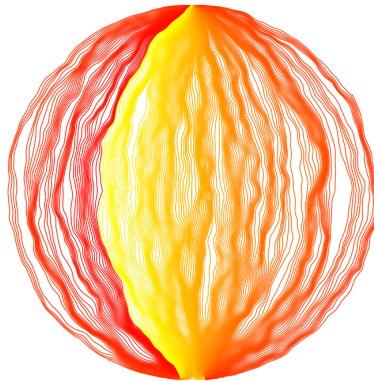


Figure 5.6: A simulation of flow line from $-i$ to i on unit disk

5.3.1 Choice of domain D

Although the numerical method to calculate the conformal mapping is possible, we prefer it to be ϕ explicit since we need not only the mapping but also its derivative and these require many calculus.

We propose a conformal mapping $\phi : \mathbb{D} \rightarrow \mathbb{H}$

$$\begin{aligned}\phi(z) &= i \left(\frac{1 - iz}{1 + iz} \right) \\ \phi'(z) &= \frac{2i}{(1 + iz)^2}\end{aligned}$$

then $\phi(-i) = 0, \phi(i) = \infty$. Therefore, all the flow lines on this domain are the flows connecting $-i$ and i .

5.3.2 Simulation of GFF on any domain

Once we fix the domain as a unit disk, the rest is to generate a GFF with null boundary condition on it. People may wonder what is the orthogonal base on it, but we would like propose another method using the decomposition of GFF.

The idea is simple : using the property of Markov domain. In detail, we sample a GFF on the square $[-1, 1]^2$ which is comparatively easy and we have stated the method in the preceding chapter, then we do harmonic extension of its boundary value on $\partial\mathbb{D}$ and we denote it by h_{Harm} . This step can be realized numerically by iterate a function with the boundary condition until it satisfies the discrete Laplace equation. Finally, as proposed by 3.4.1, $h_{\mathbb{D}} = h - h_{Harm}$ is a GFF on the disk with null boundary condition.

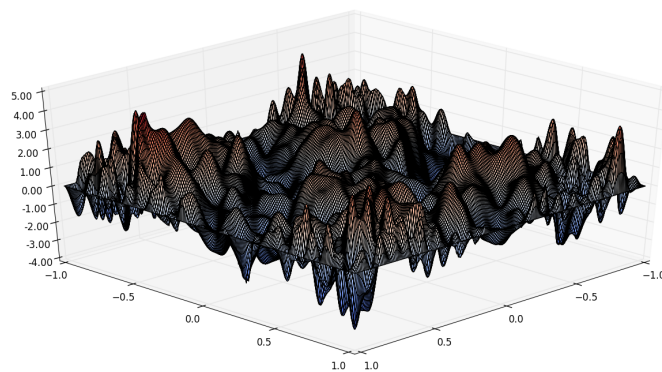


Figure 5.7: A simulation of the harmonic extension on the unit disk

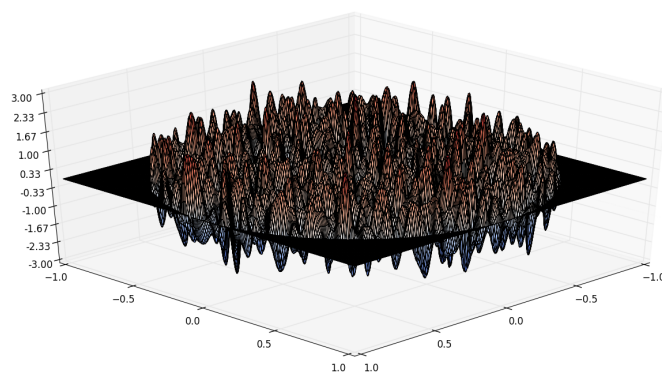
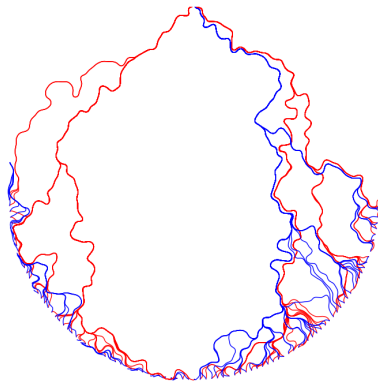


Figure 5.8: A simulation of a GFF on the unit disk by subtracting a harmonic extension from a GFF on the square $[-1, 1]^2$



6

Conclusion

In conclusion, we finish the introduction of the SLE and GFF and the its coupling.

SLE is a random set described by the random flow, and is the limit of some discrete random objects when varying the choice of κ which also decides its behavior. This fact also reveals that study about SLE can be divided into two parts : its own properties and the connection with other models. The study of the former uses Ito integration and complex analysis in for estimating the continuity in some step. The study of the connection between SLE and other models hasn't been included in this stage, but the tools could be more various. There are still many open questions to solve, for example the connection between SLE_6 and the interface of Ising model is just solved in the hexagonal situation and we believe that is should be correct in general case. The numerical part of SLE is now also largely used in physics to identify the other random curves.

GFF is a random distribution or random generalized function. We could see it as a noise added to each point of the domain but the noises on two points have a correlation. We use it to construct Liouville quantum gravity, which could be seen as the same object as Brownian map. This is not easy to see since the Brownian map has metric but without the conformal structure, while Liouville quantum gravity has a conformal structure but lacks of distance on it. The main tool to relate the two object depends on the quantum Loewner evolution which is out of the range of this report.

The imaginary geometry refers in fact the coupling between SLE and GFF and the beautiful images such at the monotony, the merging, the light cone, the SLE fan are just the performance of a interactions of several SLE coupled with the same GFF. A key technical tool in these work is local set which plays the same role as strong Markov

property in Brownian motion. The coupling appears at first between SLE_4 and the level line of GFF, latter between $SLE_\kappa(\rho)$ and the GFF with boundary condition constant in interval. We can imagine that the coupling between a variant of SLE and a GFF with general boundary condition is also possible.

Finally, we remark that the numerical simulation observes almost all the nice pictures but this supposes the convergence from discrete GFF to continuous GFF. However, there is no theory connecting the approximation of GFF between the coupling except the SLE_4 case.

Appendix A

Appendix

A.1 Riemann mapping theorem

The Riemann mapping theorem may be one of the most important theorem in complex analysis. The basic theorem is as following :

Theorem A.1.1 (Riemann mapping theorem). $\forall U \subset \mathbb{C}$ simply connected open subset, there is a unique biholomorphic $f : \mathbb{D} \rightarrow U$ such that $f(0) = z \in U, f'(0) > 0$.

We will not prove this theorem since the proof can be found in many textbook like [SS03]. This theorem tells us more than the theorem itself. In fact, the theorem can be generalized to any two simply connected open subset U, V .

Corollary A.1.1. $\forall U, V \subset \mathbb{C}$ simply connected open subset, there is a unique biholomorphic

$$h : U \rightarrow V, h(x) = y, x \in U, y \in V, h'(x) > 0.$$

Proof. To prove the existence, we suppose that $f : \mathbb{D} \rightarrow U$ and $g : \mathbb{D} \rightarrow V$ such that $f(0) = x, f'(0) > 0, g(0) = y, g'(0) > 0$, then we compose the two and get $h = g \circ f^{-1}$. Then it is a biholomorphic mapping wanted.

To prove the uniqueness, we suppose h_1, h_2 satisfy the requirement and f as defined above. Then $g_i = h_i \circ f, i = 1, 2$ defines two biholomorphic mapping satisfying $g_i(0) = y, g'_i(0) > 0$. The uniqueness of Riemann mapping theorem proves that $g_1 = g_2$, so as the equality of h_1, h_2 . \square

A.2 Gaussian space and Gaussian process

We recall some basic concepts and nice structures of Gaussian vector, Gaussian space and Gaussian process.

Definition A.2.1 (Gaussian vector). (X_1, X_2, \dots, X_n) is said Gaussian vector if and only if any linear combination of them has a Gaussian distribution.

It is easy to show that if $\{Y_n\}_{n \geq 0}$ has a law of Gaussian and converges in L^2 to a random variable Y , then Y is also Gaussian. This idea incites the definition of Gaussian space.

Definition A.2.2 (Gaussian space). A Hilbert space H is called Gaussian space if it's formed by Gaussian random variables and by the norm of L^2 . In other word, it is a closed sub-space of $L^2(\Omega, \mathcal{F}, \mathbb{P})$ formed by Gaussian random variables.

Gaussian space has a very nice structure : its independence can be characterized by inner product.

Proposition A.2.1 (Independence of Gaussian space). *Two Gaussian spaces $H_1, H_2 \subset L^2(\Omega, \mathcal{F}, \mathbb{P})$ are independent i.e $\sigma(H_1)$ and $\sigma(H_2)$ are independent if and only if they are orthogonal $H_1 \perp H_2$.*

Gaussian process is another way to generalize Gaussian vector : it could have infinite elements indexed by I .

Definition A.2.3 (Gaussian process). We define $\{X_i\}_{i \in I}$ a Gaussian process indexed by I if any finite linear combination of element is centered Gaussian.

We introduce the definition of white noise, which can be seen as Gaussian process indexed by the function in $L^2(E, \mathcal{E}, \mu)$.

Definition A.2.4 (White noise). Given a measure space (E, \mathcal{E}) and μ a σ -finite measure on it, a white noise B of intensity μ is an isometry between $L^2(E, \mathcal{E}, \mu)$ and a Gaussian space.

That is to say, $\forall f, g \in L^2(E, \mathcal{E}, \mu)$, $B(f) \sim \mathcal{N}(0, \|f\|_{L^2_\mu}^2)$ and

$$\mathbb{E}[B(f)B(g)] = \int_E f(x)g(x)\mu(dx)$$

. Finally, we give a canonical construction of white noise.

Proposition A.2.2 (Canonical construction of white noise). *We pick $\{X_n\}_{n \geq 0}$ a family of independent Gaussian centered normalized random variables in probability space $(\Omega, \mathcal{F}, \mathbb{P})$ and an orthogonal normal basis $\{e_n\}_{n \geq 0}$ of $L^2(E, \mathcal{E}, \mu)$. Then the mapping $B : L^2(E, \mathcal{E}, \mu) \rightarrow (\Omega, \mathcal{F}, \mathbb{P})$*

$$B\left(\sum_{n \geq 0} \alpha_n e_n\right) = \sum_{n \neq 0} \alpha_n X_n$$

defines a white noise.

A.3 Spectral of Laplace operator

We recall some important properties of spectral theory of Laplace operator.

Theorem A.3.1 (Compact operator). *Given $D \subset \mathbb{R}^d$ relative compact, then $(-\Delta)^{-1} : L^2(D) \rightarrow L^2(D)$ is a linear, bounded, compact, symmetry operator with discrete eigenvalues*

$$0 \leq \lambda_1 \leq \lambda_2 \leq \dots$$

where the only possible accumulative point is 0.

Remark. $(-\Delta)^{-1}$ sends a L^2 function to $H_0^1(D)$ and we know the compact injection from $H_0^1(D)$ to $L^2(D)$, so it's a compact operator from $L^2(D)$ to $L^2(D)$.

An important property is that we can construct an orthogonal normal basis by the eigenvector of $(-\Delta)^{-1}$.

Corollary A.3.1 (Orthogonal normal basis). *The eigen-vectors $\{l_n\}_{n \geq 0}$ associated to $(-\Delta)^{-1}$*

$$(-\Delta)^{-1} l_n = \lambda_n l_n$$

form an orthogonal normal basis of $L^2(D)$.

A very simple calculus show that if $f \in H_0^1(D)$

$$\begin{aligned} \|f\|_{\nabla}^2 &= \left\langle \sum_{n=1}^{\infty} \langle f, l_n \rangle l_n, (-\Delta)^{-1} \sum_{n=1}^{\infty} \langle f, l_n \rangle l_n \right\rangle \\ &= \sum_{n=1}^{\infty} \langle f, l_n \rangle^2 \lambda_n \end{aligned}$$

This inspires us to define a general Soblev space $H_0^s(D)$ using this basis and this definition is equivalent with other method like transform of Fourier.

Definition A.3.1 (General Soblev space). A general distribution $f \in H_0^s(D)$ if

$$\|f\|_{H_0^s(D)}^2 = \sum_{n=1}^{\infty} \langle f, l_n \rangle^2 \lambda_n^s$$

.
Last theorem is a famous theorem of Weyl about the estimation on the eigenvalue of $(-\Delta)^{-1}$. An easy version can be seen from the one dimension Laplace equation defined on interval.

Theorem A.3.2 (Weyl). *The eigenvalue has an asymptotic increment*

$$\lim_{n \rightarrow \infty} \frac{\lambda_n^{d/2}}{n} = \frac{(2\pi)^d}{|D|\alpha(d)}$$

. *Especially, when $d = 2$, we have $\lambda_n \asymp n$.*

A.4 Phase of Bessel process

Bessel process is a random process of $X_t = |B_t|$ where B_t is a Brownian motion in \mathbb{R}^d . It has some interesting properties. One of the most important properties is that its phase depends on the dimension.

Theorem A.4.1 (Recurrence of Bessel process). *When $0 < d < 2$, the d -dimensional Bessel process is recurrent, while $d \geq 2$, it is transient.*

Proof. Applying formula d'Ito, we obtain

$$dX_t = \frac{d-1}{2X_t} dt + dB_t.$$

To kill the drift, we search for a local martingale X^{2-d} when $d \neq 2$

$$\begin{aligned} d(X^{2-d}) &= (2-d)X^{1-d}dX_t + \frac{(2-d)(1-d)X^{-d}}{2}dt \\ &= \frac{(2-d)(d-1)X_t^{1-d}}{2X_t}dt + (2-d)X_t^{1-d}dB_t + \frac{(2-d)(1-d)X^{-d}}{2}dt \\ &= (2-d)X_t^{1-d}dB_t \end{aligned}$$

Using the theorem of optional stopping time

$$\begin{aligned} \mathbb{E}[X_{t \wedge \tau_a \wedge \tau_b}^{2-d}] &= \mathbb{E}[X_0^{2-d}] \\ \Rightarrow \mathbb{P}[\tau_a < \tau_b] &= \frac{b^{2-d} - X_0^{2-d}}{b^{2-d} - a^{2-d}}. \end{aligned}$$

We take $b \rightarrow \infty, a \rightarrow 0$ and obtain two cases

$$\begin{aligned} d < 2, \quad \lim_{b \rightarrow \infty, a \rightarrow 0} \mathbb{P}[\tau_a < \tau_b] &= 1 \\ d > 2, \quad \lim_{b \rightarrow \infty, a \rightarrow 0} \mathbb{P}[\tau_a < \tau_b] &= 0. \end{aligned}$$

The critical case $d = 2$ should be treated with another local martingale $\log X_t$ with the similar routine

$$d = 2, \quad \lim_{b \rightarrow \infty, a \rightarrow 0} \mathbb{P}[\tau_a < \tau_b] = \lim_{b \rightarrow \infty, a \rightarrow 0} \frac{\log b - \log X_0}{\log b - \log a} = 0.$$

In conclusion, $d \geq 2$, the Bessel process is transient, while $0 < d < 2$ the process is recurrent. \square

Remark. This property means that 1D-Brownian motion is recurrent for while it is transient for greater dimension. Precise description for 2D-Brownian motion is that the trace almost surely will not come back to the origin but any small neighborhood around it.

Appendix B

Oberwolfach

This is a quick part version of the note recorded during a week of seminar organized by Jason Miller and Scott Sheffield in Oberwolfach. The first part is a review of the lectures given by different researchers. The second part is about the open questions. The third part is some personal thinking.

B.1 Random geometry review

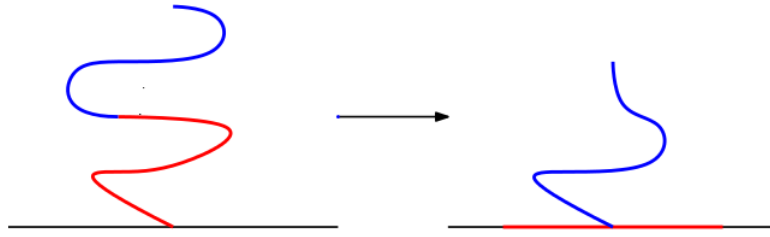
B.1.1 SLE

The theory of SLE is nowadays very familiar by many researchers in probability. It uses the Loewner evolution to capture the behavior of a growing random curves or sets. It is much studied at the beginning of 21th century and proved sucess but now its study is more related to LQG theory. The interest is that the random growing objects are always fractal, but conformal maps require only that the set is simply connected.

Various versions of SLE is developed such as $SLE_\kappa(\rho)$ [Dub09] [Dub05], which adds some force point at the boundary and it changes the behavior of SLE curves. These varied version SLE proves important in LQG theory.

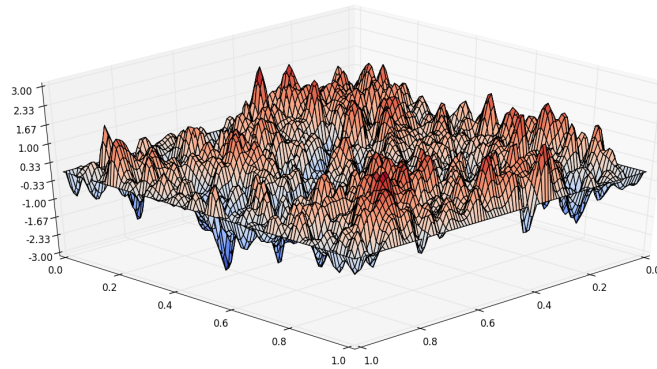
B.1.2 GFF/ γ -LQG

The GFF and LQG may be the key concept of the one week seminar. Although these two ideas are much used in the series of works by the team of Sheffield, some definition isn't so well written in the paper. On one hand, sometimes to make a mathematical concept as a physical object, we should not be so rigorous, however mathematicians always hope it more close to the classical concepts.



In fact, GFF can be treated as a $H^1(D)$ indexed Gaussian process. But to treat it more precisely, it should be a random variable value in $H^{-\epsilon}(D)$. [Aru15] may be one perfect reference : it develops all the theory of GFF as a standard Brownian motion in two dimension and starts to reformulate an important technique of local set. Local set is a technique like strong Markov property, but its behavior is more complicated due to the interface. [ASW17] has studied some typical local sets and some other reviews will come in the future.

On the other hand, LQG as a random object taking value as a measure, is sometimes called quantum measure, Liouville measure, quantum length(at boundary) etc. It has also other constructions like by CLE_4 and local set technique [APS17].

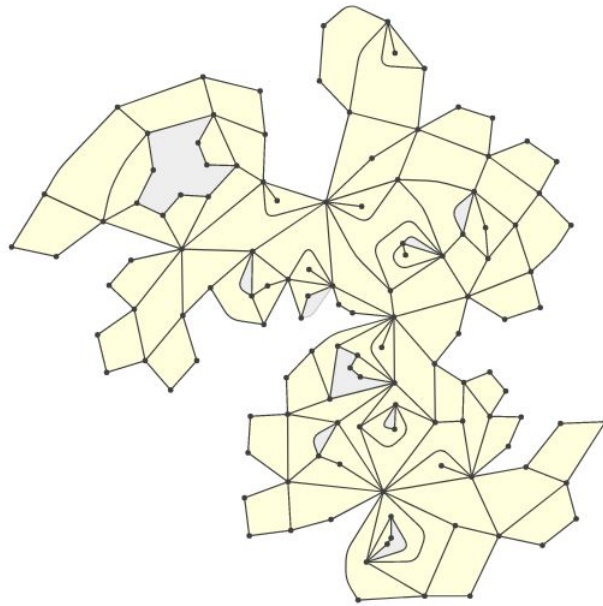


B.1.3 Random maps

Random maps is another famous random object studied much. Without talking about the physics background, we can just see it as a scaling limit of discrete models.

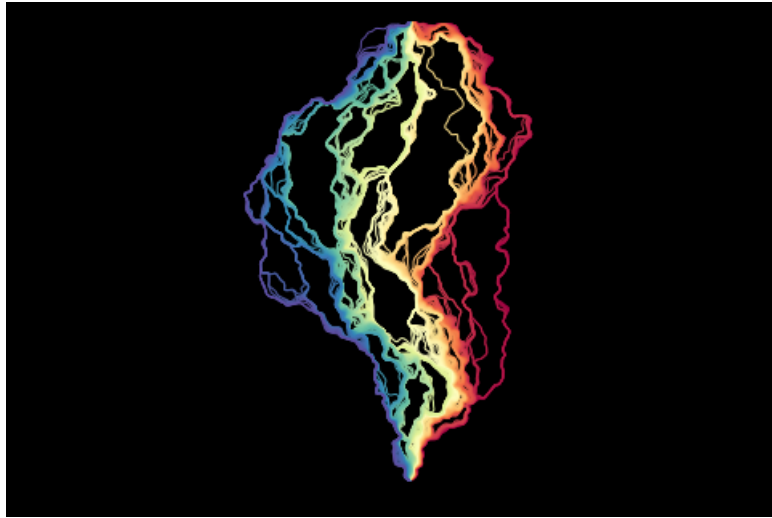
Random maps have general two types of convergence, Gromov-Hausdorff convergence [M⁺13] [LG⁺13] and local limit. In Gromov-Hausdorff convergence, the technique invented in this area especial by French school is very powerful and robust, and we have many extension result like random maps with boundary, with genus etc. In local limit side, the Markov property and peeling process has perfect counter in LQG and inspires the study of quantum zipper etc.

We hope to generalize the results of random maps further in future. But the appearance of mating of tree induces us to think about the relationship between them ?



B.1.4 SLE/GFF coupling

The technique of SLE/GFF coupling [MS16a] [MS⁺16d] [MS16b] has many derived versions and its most important contribution in the LQG theory is the imaginary geometry(see the beautiful image in the report, it does have sense more than just a nice simulation) The imaginary geometry tells us in fact, LQG may be decomposed by the reunion of flow, that's the part of motivation of the mating of trees. However, to generalize a general boundary condition coupling, it requires work. Besides the work mentioned, [PW15] studies a more general boundary condition coupling.



B.1.5 Quantum surface

This may be one of the most difficult part the in work of Jason Miller and Scott Sheffield. In their talk, they mention the terminology like quantum wedges, quantum cones, quantum disks everywhere and usually makes people puzzled.

To understand it, I think the motivation is more important than the maths part : why we invent these objects ? Let's draw some connection of peeling process. In peeling process [Bud16], [Cur15], we peel from the origin towards a targeted point with two operations, peeling the outside area and filling the hull if the genus happens. The domain Markov property makes it very nice when we choose the critical probability of the percolation : the boundary increment has a law as Markov transition and we fill in the hull with a triangulation.

On the LQG sides, it is the same idea : the zipper up (a SLE path) is like the exploration of random maps and we have to define how to fill in the bubble by defining the GFF in it, which plays the same role as filling the hull a triangulation.

So, all the work like welding, quantum wedges, quantum cones are trying to make it explicit. However, the complicated formula sometimes makes people a little afraid and there is indeed some fine part to treat. Some notation seems tedious, for example the definition of weight of quantum makes so little sense. In a word, we just consider it as a continuous version of filling random triangulation.

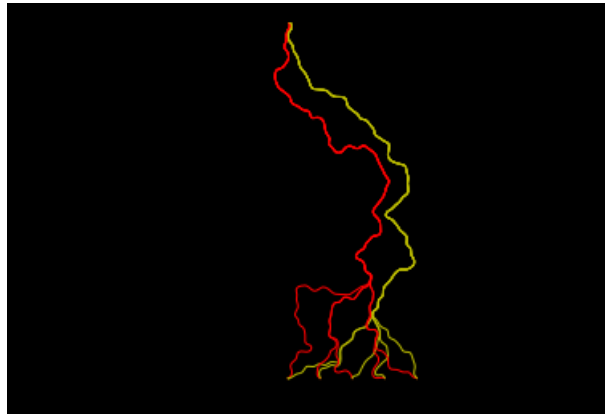
B.1.6 Mating of trees

To make this idea in [DMS14] understood and more popular is the goal of this seminar. Generally, when we define two different equivalent relation on two trees and glue them together, this will be graph coded by two trees. One we pass to the limit, the CRT convergence makes sense of some distance on the sphere. This is the idea of mating of trees.

In LQG, the structure of trees comes from the flow line : from one point, it can generate two flow lines of degree $-\frac{\pi}{2}, \frac{\pi}{2}$, the coalescence phenomena generates two trees. Then we can reverse the duality of counter flow line to recover the order and length of the Brownian motion of the two trees - we know it is a Brownian motion since the left boundary length and right boundary length has independent increment and scaling invariant.

Reversely, we can also prove that the two trees determine a LQG and decorated SLE. In this side, we have to embedding the gluing real tree into a disk to see that they decide a LQG and SLE. Some tool like Efron-Stein is used in this proof of conformal mapping.

We remark at last the Efron-Stein method is very powerful in the proof of embedding and the proof of Brownian map determining LQG uses also this idea. So, we study the scaling limit of this structure, what we need is just a bijection coded by two random walk. Many research on this direction has been produced like [HS16], [KMSW15], [LSW17].



B.2 Open questions

Here I record some questions recorded in this week.

B.2.1 Finding bijections

The technique of mating of trees prove very quick, so can we find other random maps decorated models such that "random map + decorated model \rightarrow LQG + SLE" in the sense of peanosphere ?

B.2.2 Gromov-Hausdorff vs Peanosphere vs Embedding convergence

We have three types of convergence as in title. We didn't talk about local limit since it doesn't apply normalization. Gromov-Hausdorff convergence is used a lot in Brownian trees/lamination/maps/maps with boundary/disks and requires a very strong bijection. Embedding convergence is also once used in other context, in the topology of Carathéodory and the Efron-Stein estimation is also very robust. Peanosphere topology of mating of trees technique requires also a bijection but a little weaker. Question is that can we pass one type of convergence to another ? Or in some specific situations ?

B.2.3 Mismatch

One technique necessary in all the series of work is the coupling of GFF and SLE $\kappa = \gamma^2$. Scott Sheffield asks whether we can treat the situation without this coupling ? Of course, a SLE is always allowed on LQG, but we will not have so nice local set technique.

B.2.4 String theory and Yang-Mills

What Scott Sheffield hopes to solve ? To reformulate Yang-Mills and string theory. Informally speaking, Yang-Mills is some random walk of matrix multiplication and we hope to study its trace behavior. The string theory part, physicists think the move of the string is just like the random surface. **Three big difficulty** : 1, LQG to dimension 4. 2, Pass the mismatch situation. 3. Treat the LQG with many many genus. Scott thinks maybe 1 is the easiest one.

Some concrete question can be studied : 1, Two Brownian snakes with head in the same x axis. 2, The left boundary length and right boundary length of the flow line in mismatch case (a couple of correlated Levy tree ?).

B.2.5 Branching/Coalescence

What's the behavior of branching or coalescence of the two trees in LQG ? Can we use it to code the LQG/Brownian map ?

B.2.6 Open question everyone knows

Some famous open question everyone knows like the convergence of flow line, DLA model on the lattice etc.

B.3 Personal thinking

The big project of Scott Sheffield is sometimes more like construction a bridge between mathematics and physics, that may be the reason why the article is very big and sometimes hard to understand. For physicists, the existence of an object with some property can be imagined and we can give them an mathematical object, but if they need other property or operation on this object, we have to treat it more carefully. The series of work in LQG is like it : we find different random object to describe all the role in a big frame.

Anyway, this program attracts many people to continue improve the maths part and inspires the work of other researchers. The tools and objects invented in the frame are also interesting and may have other surprising applications.

Bibliography

- [APS17] Juhan Aru, Ellen Powell, and Avelio Sepúlveda. Approximating liouville measure using local sets of the gaussian free field. *arXiv preprint arXiv:1701.05872*, 2017.
- [Aru15] Juhan Aru. *The geometry of the Gaussian free field combined with SLE processes and the KPZ relation*. PhD thesis, Ecole normale supérieure de lyon-ENS LYON, 2015.
- [ASW17] Juhan Aru, Avelio Sepúlveda, and Wendelin Werner. On bounded-type thin local sets of the two-dimensional gaussian free field. *Journal of the Institute of Mathematics of Jussieu*, pages 1–28, 2017.
- [B⁺17] Nathanaël Berestycki et al. An elementary approach to gaussian multiplicative chaos. *Electronic Communications in Probability*, 22, 2017.
- [Bef12] Vincent Beffara. Schramm-loewner evolution and other conformally invariant objects “probability and statistical physics in two and more dimensions”.(d. ellwood, c. newman, v. sidoravicius and w. werner, editors). *Proceedings of the Clay Mathematics Institute Summer School and XIV Brazilian School of Probability (Buzios, Brazil), Clay Mathematics Proceedings*, 15:1–48, 2012.
- [Ber15] Nathanaël Berestycki. Introduction to the gaussian free field and liouville quantum gravity. *Lecture notes, available on author’s webpage*, 2015.
- [Bud16] Timothy Budd. The peeling process of infinite boltzmann planar maps. *The Electronic Journal of Combinatorics*, 23(1):P1–28, 2016.
- [Cur15] Nicolas Curien. A glimpse of the conformal structure of random planar maps. *Communications in Mathematical Physics*, 333(3):1417–1463, 2015.

- [DMS14] Bertrand Duplantier, Jason Miller, and Scott Sheffield. Liouville quantum gravity as a mating of trees. *arXiv preprint arXiv:1409.7055*, 2014.
- [DS11] Bertrand Duplantier and Scott Sheffield. Liouville quantum gravity and kpz. *Inventiones mathematicae*, 185(2):333–393, 2011.
- [Dub05] Julien Dubédat. Sle (κ, ρ) martingales and duality. *Annals of probability*, pages 223–243, 2005.
- [Dub09] Julien Dubédat. Sle and the free field: partition functions and couplings. *Journal of the American Mathematical Society*, 22(4):995–1054, 2009.
- [Gar12] Christophe Garban. Quantum gravity and the kpz formula. *arXiv preprint arXiv:1206.0212*, 2012.
- [Gol] Françoise Golse. Distributions, analyse de fourier, équations aux dérivées partielles.
- [HS16] Nina Holden and Xin Sun. Sle as a mating of trees in euclidean geometry. *arXiv preprint arXiv:1610.05272*, 2016.
- [Kah85] J-P Kahane. *Sur le chaos multiplicatif [On the multiplicative chaos]*. Université de Paris-Sud. Département de Mathématique, 1985.
- [Kah87] Jean-Pierre Kahane. Multiplications aléatoires et dimensions de hausdorff. *Ann. Inst. H. Poincaré Probab. Statist.*, 23(2):289–296, 1987.
- [Ken07] Tom Kennedy. A fast algorithm for simulating the chordal schramm–loewner evolution. *Journal of Statistical Physics*, 128(5):1125–1137, 2007.
- [KMSW15] Richard Kenyon, Jason Miller, Scott Sheffield, and David B Wilson. Bipolar orientations on planar maps and sle $_{\{12\}}$. *arXiv preprint arXiv:1511.04068*, 2015.
- [KP76] J-P Kahane and Jacques Peyriere. Sur certaines martingales de benoit mandelbrot. *Advances in mathematics*, 22(2):131–145, 1976.
- [Law07] Gregory F Lawler. Schramm-loewner evolution. *arXiv preprint arXiv:0712.3256*, 2007.

- [Law08] Gregory F Lawler. *Conformally invariant processes in the plane*. Number 114. American Mathematical Soc., 2008.
- [LG⁺13] Jean-François Le Gall et al. Uniqueness and universality of the brownian map. *The Annals of Probability*, 41(4):2880–2960, 2013.
- [LSW17] Yiting Li, Xin Sun, and Samuel S Watson. Schnyder woods, sle (16), and liouville quantum gravity. *arXiv preprint arXiv:1705.03573*, 2017.
- [M⁺13] Grégory Miermont et al. The brownian map is the scaling limit of uniform random plane quadrangulations. *Acta mathematica*, 210(2):319–401, 2013.
- [MS13] Jason Miller and Scott Sheffield. Imaginary geometry iv: interior rays, whole-plane reversibility, and space-filling trees. *arXiv preprint arXiv:1302.4738*, 2013.
- [MS15] Jason Miller and Scott Sheffield. Liouville quantum gravity and the brownian map i: The qle (8/3, 0) metric. *arXiv preprint arXiv:1507.00719*, 2015.
- [MS16a] Jason Miller and Scott Sheffield. Imaginary geometry i: interacting sles. *Probability Theory and Related Fields*, 164(3-4):553–705, 2016.
- [MS16b] Jason Miller and Scott Sheffield. Imaginary geometry iii: reversibility of SLE _{κ} for $\kappa \in (4, 8)$. *Annals of Mathematics*, 184(2):455–486, 2016.
- [MS16c] Jason Miller and Scott Sheffield. Liouville quantum gravity and the brownian map ii: geodesics and continuity of the embedding. *arXiv preprint arXiv:1605.03563*, 2016.
- [MS⁺16d] Jason Miller, Scott Sheffield, et al. Imaginary geometry ii: Imaginary geometry ii: Reversibility of SLE _{κ} ($\rho_1; \rho_2$) for $\kappa \in (0, 4)$. *The Annals of Probability*, 44(3):1647–1722, 2016.
- [MS⁺16e] Jason Miller, Scott Sheffield, et al. Quantum loewner evolution. *Duke Mathematical Journal*, 165(17):3241–3378, 2016.
- [Pol81] Alexander M Polyakov. Quantum geometry of bosonic strings. *Physics Letters B*, 103(3):207–210, 1981.

- [PW15] Ellen Powell and Hao Wu. Level lines of the gaussian free field with general boundary data. *arXiv preprint arXiv:1509.02462*, 2015.
- [RS11] Steffen Rohde* and Oded Schramm. Basic properties of sle. *Selected Works of Oded Schramm*, pages 989–1030, 2011.
- [RV⁺14] Rémi Rhodes, Vincent Vargas, et al. Gaussian multiplicative chaos and applications: a review. *Probability Surveys*, 11, 2014.
- [She07] Scott Sheffield. Gaussian free fields for mathematicians. *Probability theory and related fields*, 139(3):521–541, 2007.
- [SS03] Elias M Stein and Rami Shakarchi. *Princeton lectures in analysis*. Princeton University Press, 2003.
- [SS09] Oded Schramm and Scott Sheffield. Contour lines of the two-dimensional discrete gaussian free field. *Acta mathematica*, 202(1):21–137, 2009.
- [SS13] Oded Schramm and Scott Sheffield. A contour line of the continuum gaussian free field. *Probability Theory and Related Fields*, 157(1-2):47–80, 2013.
- [Wer04] Wendelin Werner. Part ii: Random planar curves and schramm-loewner evolutions. *Lectures on probability theory and statistics*, pages 107–195, 2004.